Bachelor Thesis

Degree Project in
Geology 15 hp

Petrological and Structural Characterization of an Older Rock Suite in the Triabo-Area, South of Virserum, Småland

Lucas Vikdahl

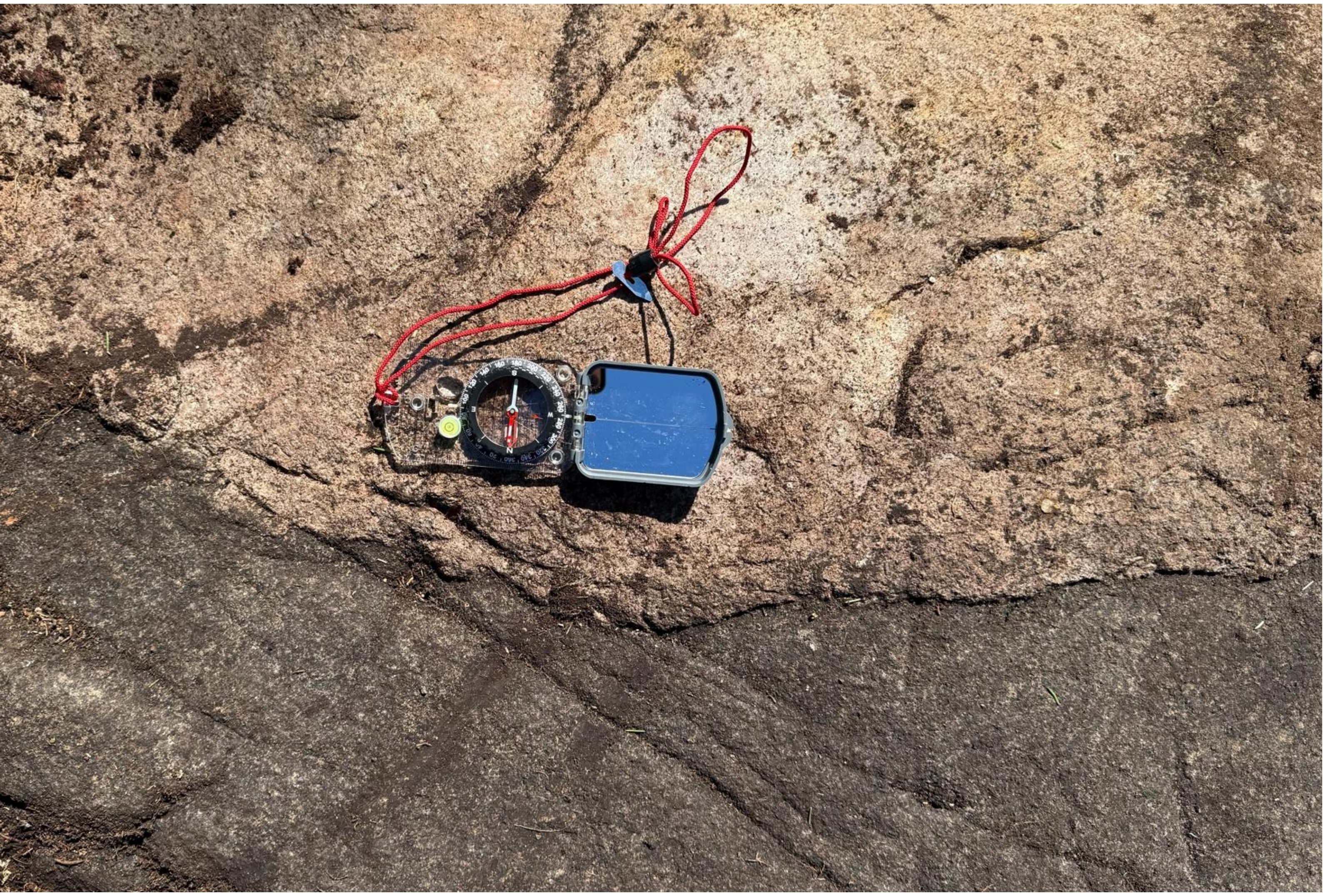

Stockholm 2025
Department of geological science
Stockholm University
SE-106 91 Stockholm

ABSTRACT

This study investigates lithological and structural relationships at the tectonic boundary between the Oskarshamn Jönköping Belt (OJB) and the Småland Värmland Belt (SVB) in southern Sweden. The aim was to determine whether specific lithological units in the field area south of Virserum reflect an OJB origin, belonging to the SVB or indicate contributions from both. To characterize the local lithologies was field mapping, petrographic analysis and density and susceptibility measurements used.

Results indicate that the older granitoid (sample LV25040) unit formed from OJB magmatism, was later subjected to SVB deformation where partial melting was induced. Sample (LV25016) reveals evidence of partial OJB derived origin, exhibiting hybrid composition, melt flow related textures and shows intrusive relationships with the surrounding lithologies.

The resulting classification of the rock is that of an anatectic melt LV25016, derived from the partial melting of the old granitiod LV25040 and hybridized through interaction with adjacent lithologies, incorporating mafic components. The results help to refine the current understanding of crustal processes in southern Sweden and support improved correlation between adjacent structural domains.

Table of Contents

1. INTRODUCTION

1.1 Aim and Research Questions

The bedrock of southern Sweden hosts a complex lithological region and is defined by a series of major tectonic belts. Of interest is the Tönshult shear zone which marks a boundary between the older Oskarshamn Jönköping Belt (OJB) and the younger Småland Värmland Belt (SVB). Although OJB both and SVB domains have undergone extensive mapping, uncertainties remain regarding the characteristics and correlations of specific lithological units. This study targets this transition zone south of Virserum, aiming to contribute to regional geological interpretations. With the aim to describe, and petrographically distinguish, the unresolved geological units, believed to be a section of Oskarshamn-Jönköping Belt (OJB). To verify if these rocks are a part of or differ from surrounding units of the Småland-Värmlands Belt (SVB), will the focus of the work revolve around a characterization of the rock's mineral compositions, metamorphism, and deformation features.

The study addresses three main questions:
(1) What are the mineralogical and petrographic characteristics of the samples believed to belong to the OJB in the study area?
(2) How do the metamorphic and structural features of these rocks compare to those of the encompassing SVB units?
(3) Do the differences observed in the samples composition and texture support the interpretation that OJB and SVB represent separate tectonic units, or do they reflect the same evolving crustal system?

1.2 Geological Background

1.2.1 Fennoscandian Shield and Svecofennian Orogeny

Hosted on the northern portion of the Baltic shield, the Fennoscandian shield encompasses Finland, northwest Russia (Kola and Karelia), Norway and the study's focal point, Sweden. Built on a foundation of Archean and Proterozoic crust, the Fennoscandian shield qualifies as one of earth's ancient cratons. The cratons formation primarily took place during the Paleoproterozoic. Episodes of crustal accretion, subduction and magmatism contributed to its make up. The most prominent crustal growth occurred around 1.9-1.86 Ga and is referred to as the Svecofennian Orogeny. During this time, convergence of island arcs and related tectonism led to the formation of extensive juvenile crust (Lahtinen et al., 2005).

1.2.2 Transscandinavian Igneous Belt (TIB)

In a later stage of its development, the Svecofennian orogeny was subjected to large felsic intrusion processes. This intrusive episode formed the Transscandinavian Igneous Belt (TIB), representing a significant episode of continental crust formation in Fennoscandian. The TIB covers a distance of over 1500 km, from Lofoten in northern Norway to Blekinge in southern Sweden (Gorbatschev & Bogdanova, 1993).
TIB consists mainly of granitoid rocks and rhyolitic volcanics. The granitoids typically show either monzogranitic composition, a roughly balanced mix between quartz, K-feldspar, and plagioclase, or granodioritc composition comprising of the same constituents but with a higher

ratio of plagioclase than K-feldspar. The rhyolitic volcanic rocks represent the extrusive equivalent of the felsic intrusions and are most commonly observed in central Sweden, while they are rare or absent in the northern parts of TIB.
The composition and origin of the TIB granitoids change along its length. In the north is TIB magmatism associated with tectonic events related to subduction, this produce I-type (igneous arc) geochemical signatures. Exhibiting less evolved composition, high quantity of hydrous minerals (amphibole and biotite) and indications for partial melting of lower crust or mantel derived sources is observed. Towards the south does the granitoids change to A-type (anorogenic) characteristics, increasing the magmatic differentiation. These rocks will show an enrichment in alkali elements, including sodium (Na) and potassium (K), these is a signature that is interpreted to have formed from more evolved magmas rich in silica. Likely formed during a post orogenic extensional phase (Högdahl et al., 2004)

1.2.3 Småland-Värmland Belt (SVB)

The Transscandinavian Igneous Belt TIB is subdivided into phases related to the age of the granitoid intrusions. Over a span of approximately 200 million years between around 1860 to 1660 Ma, these intrusions are grouped into three episodes, TIB-0 (1860-1840 Ma), TIB-1 (1810-1770 Ma) and TIB-2/3 (1720-1660 Ma.) The southern section of TIB is coupled to the TIB-1episode and commonly known as the Småland-Värmland Belt (SVB) (Högdahl et al., 2004; Mansfeld, 2024)
The SVB covers substantial portion of southeastern Sweden and exhibit a broad spectrum of igneous rocks. Thes range from mafic gabbro and norite, through intermediate monzonite and granodiorite, to felsic granite and rhyolitic volcanics. A more specific coverage of the lithologies can be observed in (Figure 1). The formation of these rocks is interpreted to reflect a continental margin subduction setting, as indicated by their high quartz and feldspar rich subalkaline compositions. There is a geochemical diversity within the SVB and the processes bringing these attributes are magma mixing and magmatic fractionation between mafic and felsic magmas (Å. Johansson, 1988; Högdahl et al., 2004).

1.2.4 Oskarshamn-Jönköping Belt (OJB)

Enclosed within the Småland-Värmland Belt (SVB), a distinct geological difference in both composition and age marks the presence of the approximately 150 km east to west trending Oskarshamn-Jönköping Belt (OJB) (Figure 1). Dated to an age of around 1.83-1.82 Ga, the OJB predates SVB and the TIB-1 episode, indicating a separate formation history interpreted as a subduction related volcanic arc setting. This definition is supported by the belt's lithology, mainly consisting of mafic to intermediate volcanic and plutonic rocks, including gabbro, diorite, tonalite, and granodiorite, many of which exhibit foliation (R. Johansson et al., n.d.). Geochemical signatures consistent with a mantle wedge derived origin are included within OJB. The unit Fröderyd Group within OJB further supports the subduction related interpretation, its geochemistry can be coupled to a Mid Ocean Ridge Basalt (MORB) like genesis, suggesting for- ark or a back-ark rift setting (Mansfeld et al., 2005).

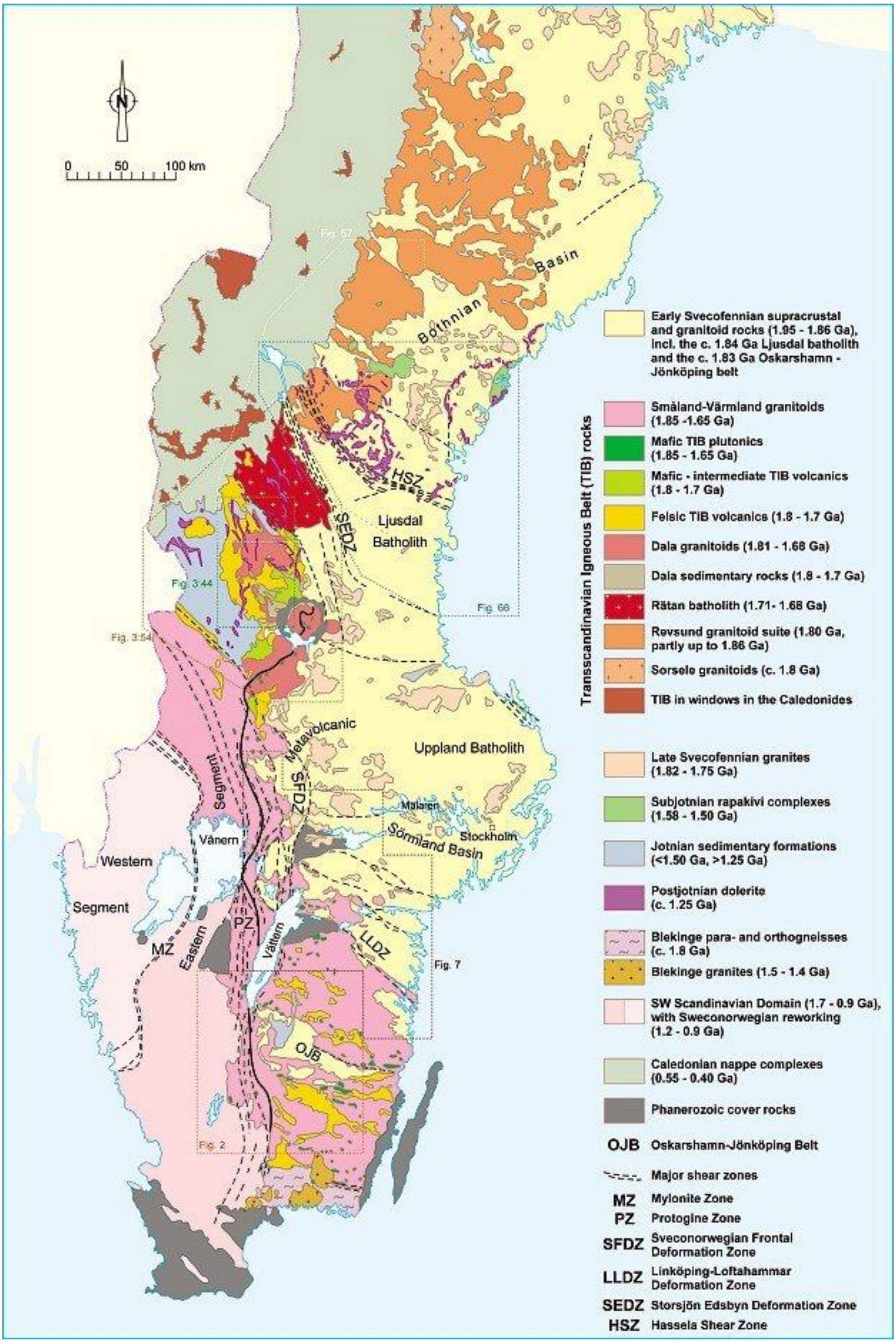

Figure 1. *Geological overview map of the Transscandinavian Igneous Belt in central and southern Sweden, showing the Småland-Värmland Belt (SVB) and Oskarshamn-Jönköping Belt (OJB). The study area lies near the southern boundary of the OJB. Source:(Högdahl et al., 2004)*

1.2.5 Tönshult Shear Zone

The Tönshult shear zone is nestled in between two geological domains, to the north it is flanked by the Oskarshamn-Jönköping Belt (OJB) and to the south the Småland-Värmland Belt (SVB) (Figure 2). The shear zone is approximately 5 km wide and trends in a WNW-ESE direction. A clear north to south overprint of the rocks is seen, diminishing in intensity away from the shear zones core. When going south from the northern part, OJB tonalites begin transitioning into strongly deformed rocks, representing ether highly deformed granitoids or deformed crystal-rich volcanic rocks. Farther south, past the most intensely deformed zone, felsic porphyries belonging to SVB become more dominant. Continuing southward, the Tönshult shear zone ends in equigranular fine to medium crystalline granitoids typical of the SVB (Mansfeld & Sturkell, 1996). The northern segment of the shear zone strikes at 80-100°, while the southern segment consists of two distinct shear structures. A ductile shear zone trending 100-120° and a younger, ductile to brittle shear zone which cuts narrowly trough otherwise undeformed bedrock (R. Johansson et al., n.d.; Mansfeld & Sturkell, 1996).

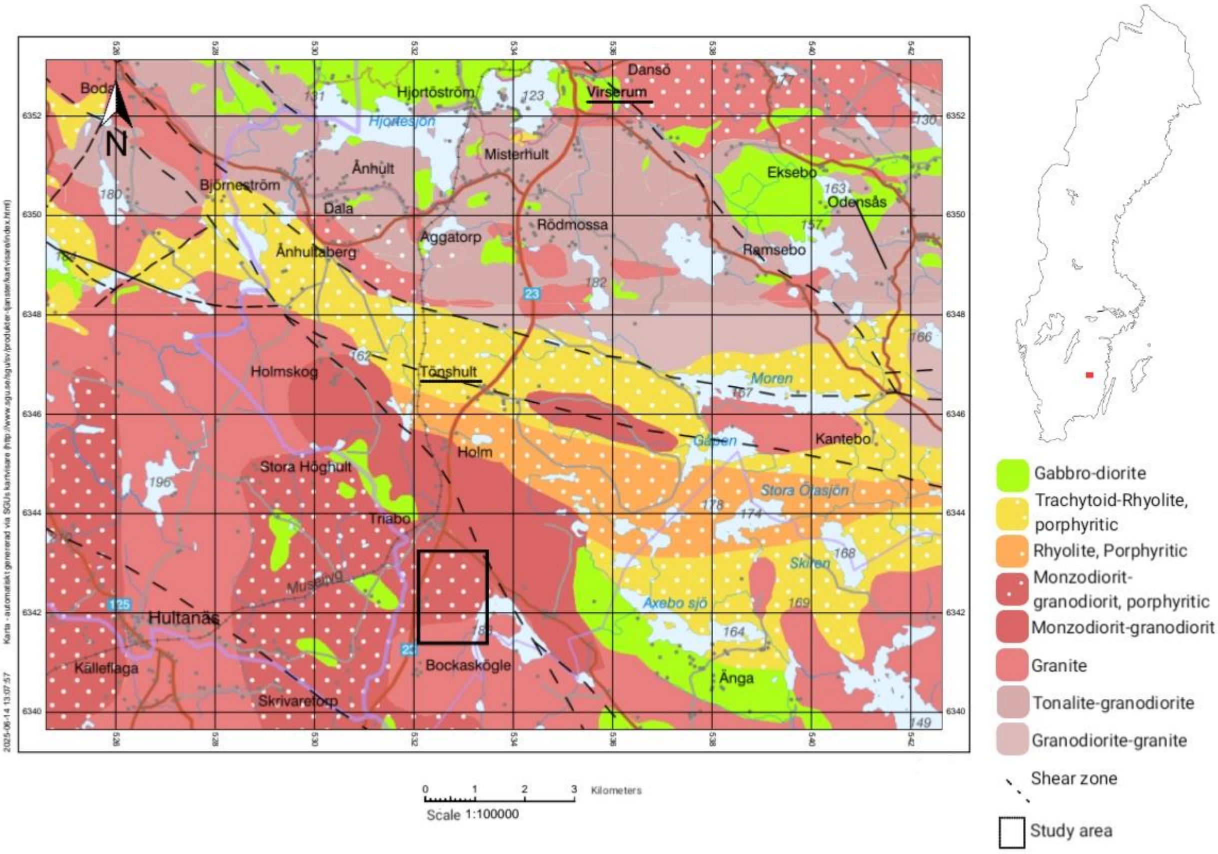

Figure 2. *Modified SGU bedrock map showing the study are south of Virserum. The Tönshult shear zone separates Oskarshamn-Jönköping Belt (OJB) to the north from Småland-Värmland Belt (SVB) lithologies to the south. Source: (SGUs Kartvisare, n.d.)*

1.3 Study Area and Local Geology

The research locality is found in southeastern Småland, 12km south of Virserum and 4 km south of the Tönshult shear zone. The area in focus is between the lake Triasjön and local road network, as shown in (Figure 2). The terrain is sloping gently toward the northeast, with elevation going from 220 - 200 meters above sea level. The plant cover is represented by managed forests with clear- cut irregularly distributed open areas, helping to expose local bedrock (*Min Karta*, n.d.).

1.3.1 Main Lithologies of the Study Area

The study areas main lithologies are summarized below and is based on the legend and outcrop description from (Rontakokko & Mansfeld, 2000).

Diabase
Described as fine crystalline, dark gray, homogeneous and with an ophitic texture. Lath shaped (thin elongated and rectangular) plagioclase feldspar enclosed by pyroxene observed in the field as narrow dikes (one ~ 100m wide) with main cutting direction north to south, showcasing chilled margins.

Växjö Granite
This rock has the characteristics as an equigranular red granite. Present minerals are K-feldspar, quartz (often blueish), minor biotite and plagioclase. It is noted to be the most common rock of Småland and that it sometimes includes mafic enclaves.

Fine Crystalline Växjö granite
Appears as a light red and as a fine crystalline variety of Växjö granite. The mineral assemblage is of K-feldspar, quartz, minor biotite, and plagioclase. In outcrop, it is observed to exhibit magma mingling with partially assimilated mafic enclaves.

Dark/Gray Växjö Granite
Reddish gray to gray in color as an intermediate hybrid variant of the Växjö granitoid. Its make up consists of quartz, minor boitite, plagioclase, fine crystalline mafic enclaves and accompanied by dark purple K-feldspar phenocrysts as large as 2cm. The rock contains mafic enclaves with diffuse contacts, centimetre wide dikes of a light red granite. The composition is mentioned to be interpreted as magma mingling between Växjö granitic magma and gabbroic magma.

Filipstad Granite
Porphyritic granite with large phenocrysts and darker matrix. Minerals present in the rock are reported as red K- feldspar 2-3 cm large crystals, often mantled by pale plagioclase, darker minerals like hornblende, biotite, and little quartz. According to the recorded observations, is typical Filipstad granites rare in the Virserum area and has the tendency to resemble Växjö granite.

Småland Volcanite
Occurs as a veery fine crystalline porphyritic rhyolite with an almost glassy aphanitic texture. Described with quartz or K-feldspar phenocrysts in a aphanitic felsic matrix. Described outcrop from the Tönshult shear zone is the observed Småland volcanite showcasing an almost vertical lineation of stretched out mineral crystals.

Fine crystalline porphyritic granite or dike porphyry
Two main varieties is present, one with reddish fine crystalline matrix and 5-10mm large red brown K-feldspar phenocrysts. The other with dark fine crystalline to glassy groundmass and white feldspar phenocrysts. It is referred to as the youngest lithology, which occurs as crosscutting dikes and small bodies in surrounding Småland-Värmland granites.

Intermediate to mafic volcanic unit or porphyritic dike
Characterized by fine crystalline gray to black or green to black colors with a porphyritic texture. The rock forming minerals include phenocrysts of plagioclase or amphibole that is within a fine crystalline mafic groundmass. Regarded as a rare occurrence, based on the previous field observations in the area.

Gabbro
Known as coarse crystalline, black to dark gray rock with an equigranular texture. It contains centimetre sized pyroxene, plagioclase, and amphibole. They are encountered in both OJB and SVB during the previous mapping. Measurements of the gabbro has been noted with high magnetic susceptibility, >5000 indicating high content of ferromagnetic minerals such as magnetite.

Older Granitoid (Urgranit)
Presents as a Gray tonalitic to granodioritic rock that displays textural and compositional inhomogeneity, rich in xenoliths. The identified minerals are quartz, green to white plagioclase, reddish gray to gray K-feldspar and large amount of dark minerals. Earlier observations describe the granitoid unit in the present study area to have undergone deformation and metamorphic overprint to varying degrees, showcasing signs of magma mingling and assimilation.

Supracrustal gneiss
Appear as a gray to black, fine crystalline rock that's banded and foliated with light coloured wavy or folded bands. There is no assemblage described but assumed to have surface derived origin, namely sedimentary deposits or volcanic ash layers that has been buried and metamorphosed.

The variety of rocks showcased in the study area reflects three major geologic components. The Oskarshamn-Jönköping belt (OJB), Småland-Värmland belt (SVB) and the crosscutting Tönshult shear zone. These local tectonic and magmatic events is linked to the spatial distribution and characteristics of the regional geological units. Previous mapping of the field area outlays the occurrence of supracrustal gneiss and older granitoid (urgranit) units, corresponding to samples LV25016 and LV25040 (Figure 3). These units are typically found within the OJB, they are not common to the SVB south of the Tönshult shear zone. To test and refine previous interpretations of regional correlation between lithological units, is special focus placed on these two rock types. A characterisation of the rock's deformation, mineral composition and metamorphic grade will be made.

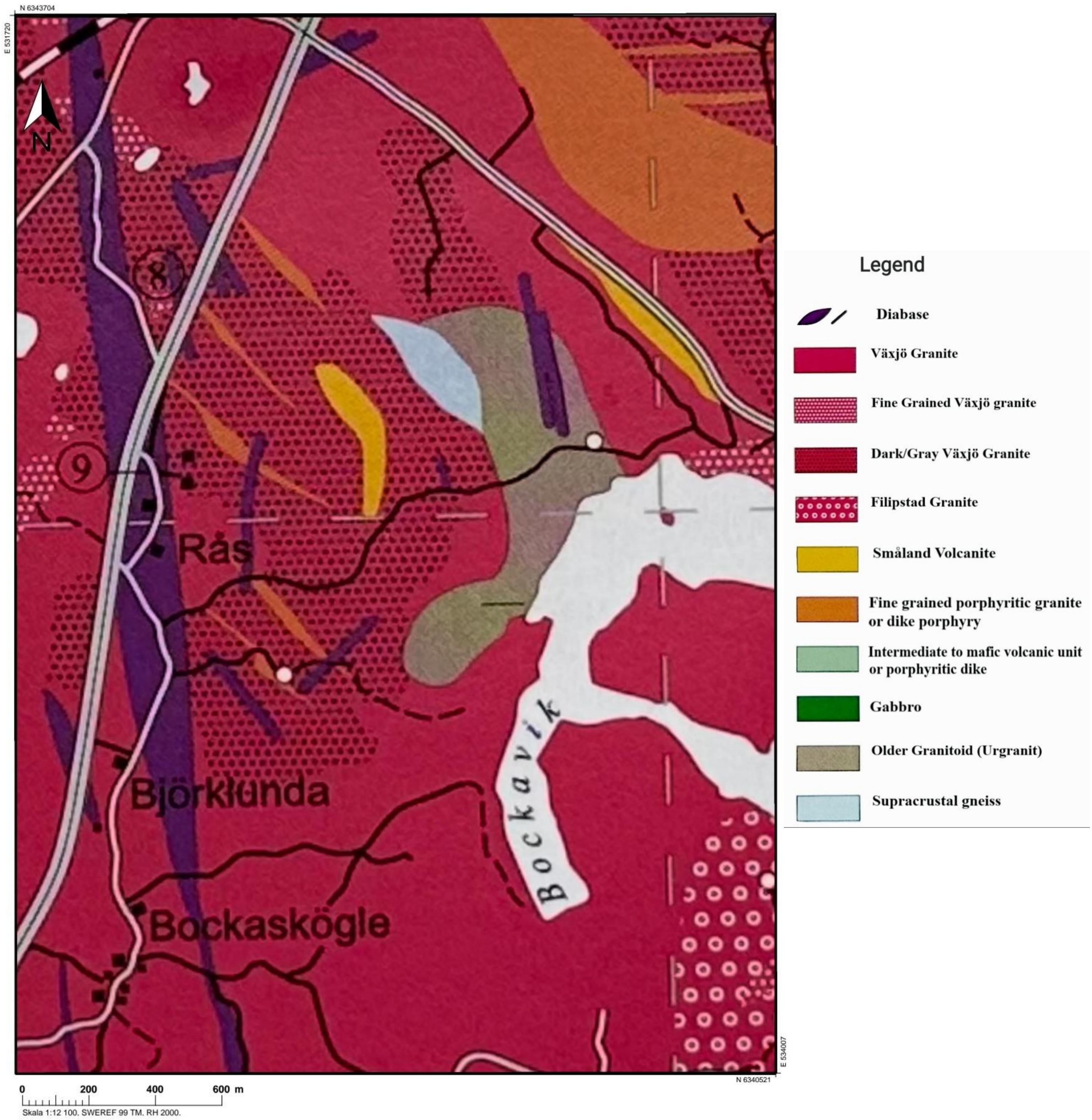

Figure 3. *Zoomed in excerpt from the geological map of the Virserum area (Mansfeld & Rantakokko, 2000), showing the mapped location of the Old granitoid (gray) and Supracrustal gneiss (light blue) units corresponding to samples LV25040 and LV25016.*

2. METHODOLOGY

A review of present maps and literature was undertaken to gain a knowledge background to help understand the local geology and guide the work forward. Key sources included regional tectonic models, geological surveys, and previous mapping work, with focus upon the two geological regions Oskarshamn-Jönköping Belt (OJB) and Småland-Värmland Belt (SVB).

2.1 Fieldwork

To gather more knowledge over the field site south of Virserum a geological mapping was undertaken. Prior the beginning of the fieldwork additional geological context was gained from participating in the Terrestrial Geophysics 2025 Fieldwork corse. On the 23rd of April, the course begins with visits to localities representing the regional lithology, this helped as an introduction to the independent work. The fieldwork was carried out in parallel with the course activities and conducted over three days spanning between the 24th to the 27th of April 2025, which yielded a total of sixty documented outcrops with varying geology. Outcrops were reached by foot and information gathered with field equipment among which geological hammer, compass clinometer, satellite GPS, elevation map from (*Min Karta*, n.d.), notebook (paper and digital), camera, susceptibility tool and fitting safety equipment protection goggles, protective gloves, reflecting west and first aid.

To determine possible bedrock localities, temporal removal of overgrowth was necessary. Uncovered and determined as a suitable outcrop, a range of geological observations was recorded. These included color, crystal size, texture, structure, magnetic susceptibility, and mineral percentage. Strike and dip (for both deformation and contact orientation) were also logged to assess intensity of deformation, helping to place the rocks in a geochronological context. Additional characteristics noted down was the coordinates, which was later used to generate a geological map with higher accuracy. When a distinct geology was observed to cover several outcrops within a limited area, optimal describing parameters were noted down once and similar units were only marked on the map to speed up the mapping. This routine was broken when a longer distance to a new outcrop was traversed or a change in the lithology seen. Lastly were samples collected in cases where outcrops displayed distinctive features that would help to explain deformation and metamorphic grade. Marked with the location name, the most promising fourteen samples were then cut and made to thin sections for further analysis.

2.2 Density Measurement

Density measurements g/cm^3 were conducted during a single fieldwork occasion, as a result could not all samples be included, since some had not yet been collected. The measurements were taken by first measuring the rock samples weight in air, followed by weighing them submerged in water. A final control measurement was taken when the rock sample had partially dried, this to ensure that no fragments had detached during measuring in the water and that the initial dry weight remained accurate. Using the formula below was the density then calculated. Density, g/cm^3 = weight in air (g) / (by weight in air - weight in water)

2.3 Petrographic Analysis

Thin sections were prepared from rock samples to determine mineral composition, textural relationship, and deformation features. This was conducted using transmitted light microscopy, utilizing the optical properties of minerals with the aid of plain polarized light PPL and cross polarized light XPL.

The analysis conducted began with the determination of modal composition, preformed visually using the area percentage method. A single mineral composition was focused on and mentally gathered at one section of the thin section, there it was determined as a percentage relative to the full area of the thin section. All minerals in each sample underwent the same method, resulting in a quantitative and comparative foundational dataset. From the proportions of the minerals was compositional trends identified, and rock types classified.

To put the sample into context was the modal estimation followed by a general petrographic description, which included crystal size, textural characteristics (example equigranular, porphyritic) and evidence of structural or alteration features. At this stage was the minerals emplacement within the sample, along with mineral textures indicative of deformation and alteration described. The QAPF diagram was used in the final step to classify the rock igneous samples, with plotting the estimated modal values into the double triangle plot. The thin sections relative abundance of the primary felsic minerals quartz (Q), alkali feldspar (A), plagioclase (P) and feldspathoids (F) were normalized from relative abundance to an accumulated percentage of 100%. Then the classification was identified and documented.

2.4 Field Mapping and Interpretation

The geological map was finalised and based on measured Sweref 99 coordinates. The coordinates were put into lantmäteriets min karta webpage and then printed out. The Interpretation of local geological coverage were biased on field notes over the sixty bedrock locations and petrographic observations, then transferred to a map. Lithological units were pared to a color then applied to interpreted covered area. Roads, houses, strike/dip, scale bar, north arrow and local names were also added to georeference the map. Descriptions of symbols and colors are explained with one attached legend that finalizes the map.

2.5 Data Integration and Synthesis

The interpretation of tectonic association was based on field observations, density measurements, petrographic analysis, and geological mapping. Comparing the different sampled units lithological characteristics (for example mineralogy, textures, and deformation features) against each other, then examined with known attributes of Oskarshamn-Jönköping Belt (OJB) and Småland-Värmland Belt (SVB) in mind. Focus was placed on the degree of deformation, alteration textures, mineral assemblages, and structural relationship between lithological units. Evaluating the attributes allowed to classify the rock units in the context of or representing OJB or SVB lithologies. Interpretations were then refined in successive steps by cross checking field relationship to observations in thin sections and structural measurements.

3. RESULTS

3.1 Field Observations and Outcrop Documentation

The field work covered an area of 3,5 square kilometres located 10 km south of Virserum between road twenty-three at west and Triasjön to the east (Figure 2). Observations were taken at foot and noted down in an elevation-based map and field notebook. The general rock types observed in the field are of granitic origin with occurring gabbroic and porphyry intrusion, all with varying deformation and composition. Overall impressions of the geology is varied, indications of magma mingling and mixing are present. Intrusion dikes and thermal alteration changes the areas rock assemblage to rock types with a hybrid transitional character that deviate from the typical norm.

3.1.1 Lithological Units

As seen in Figure 16 was each outcrop labelled with names in order they were discovered, granting outcrop one the name LV25001 and the next LV25002 and so on. LV is my initials and twenty-five is the present year. After the sample labels is the determined lithology stated, which is followed by stating the location as Sweref 99 coordinates. Lithologies were identified through field observations, focusing on color, crystal size, texture, structure, and visible mineral assemblage. Below are seven samples representing key lithologies within the study area.

LV25040 **Old granitoid** 6342209/532773
The color of the rock is gray with hints of a light pink, observed crystal size is medium crystalline between 1-5 mm, texturally of an equigranular character and with an observable but weak foliation. Estimated mineral amount are amphibole 30%, quartz 25%, plagioclase 25% and K-feldspar 20%. The outcrop is found with xenoliths of around 5-25cm and has few, up to 1cm pink granite dikes occurring sparingly.

LV25042 **Fine crystalline granitic anatectic melt** 6342322/533158
Found as fine to medium crystalline < 1-5 mm, it displays a light pink color. The rock has no foliation, finely porphyritic texture and estimated make up of plagioclase 15%, K-feldspar 45% and quartz 40%. The overall structure of the rock unit comprises of a homogeneous body, but with cutting relationships and assimilation textures to neighbouring rock (described in 2.1.2 structural and contact relationships).

LV25015 **Gabbro** (diabase) 6341811/532187
Varying dimensions of gabbroic dikes cut through the surrounding rock, spanning from 1m in width to > 25m. The color is a dark gray to green and has a crystal size that goes from medium 1-5 mm to coarse > 5 mm. There is no visible foliation, and the determined composition is of a plagioclase 30% and pyroxene/amphibole 60% mix. Its general texture is equigranular but with the addition of chilled margins, reducing the crystal sizes towards the margins. Visible on more weathered surfaces is a ophitic texture visible (Figure 4).

LV25016 **Fine crystalline intermediate anatectic melt** 6342371/533271

With a color of light grayish pink to light green and fine crystalline < 1 mm to close to medium crystalline 1-5 mm, the rock displays a texture of equigranular to seriate. It has a layered structure with varying composition and thicknesses and at a weathered section is strong deformation clearly shown (Figure 5). The composition is defined as quartz 45%, K-feldspar 35%, epidote 15% and dark minerals 5%, cutting trough this rock is 1-5 cm wide fine crystalline pink reddish dikes of granite.

LV25006 **Intermediate Växjö granite** 6342051/532403

This rock is medium to coarse with a seriate texture and a week foliation. Observable in its mainly light pink weathered surface are darker areas with pink grayish tones occurring at fresh breaks. The determined composition include plagioclase 35%, K-feldspar 25%, quartz 20% and hornblende/biotite 20%.

LV25054 **Porphyritic felsic dike** 6342603/532377

The outcrop displays a whitish pink color with an aphanitic to fine crystal matrix that showcases a porphyritic texture. Structurally it displays strong foliation that is easily seen with the alignment of phenocrysts. The phenocrysts consist of K-feldspar, which accounts for 30% of the rock's composition and the rest 70% is the aphanitic groundmass with a felsic composition.

LV25018 **Växjö granite** 6342604/533243

The color of the rock is reddish pink with a dark shade. The texture is seriate to slightly porphyritic which reflects its medium 1-5 mm to coarse > 5 mm crystal size. There is a slight deformation that is seen as a week foliation in the mineral assemblage, which is interpreted to be containing quartz 30%, K-feldspar 40% and biotite 30%.

Figure 4. *Gabbro LV25015 with ophitic texture showing needle like plagioclase crystals surrounded of pyroxene or amphibole. Pencil tip for scale, ca 0,5 cm.*

Figure 5. *Fine crystalline intermediate anatectic melt LV25016 with an assortment of colors from pink, gray to green, showing a network of a flowing irregular pattern as a schlieren texture, compass for scale, 10 cm.*

3.1.2 Structural Features and Contact Relationships

Observations from the study area identified several structural features, including alignment of platy and elongated minerals as foliation structures and shear zones. The coverage of the structures varies in intensity and orientation. Additional interactions between intrusions and later stage lithological bodies are observed.

LV25018 **Foliation** 6342604/533243

Foliation is present in almost all of the study areas lithologies, visually the deformation is most commonly seen as a subtle alignment of biotite (Figure 6). The general foliation of the study area follows the direction of the Tönshult shear zone. Additional measurements of strike and dip is found in the appendix (Table A.1)

Figure 6. *Foliation in medium crystalline granite LV25018, defined by slight planar alignment of biotite. Striking 149° and dipping 80° west, compass is parallel with foliation and is 10 cm.*

LV25041 **Shear zones** 6342186/532682

A 2,5 m wide shear zone is observed in the old granitoid (LV25040) with a strike/dip of 018/264, striking 18° and dipping 84° toward west. Within the zone there is alignment of biotite and elongated felsic streaks of quartz and feldspar, all minerals show deformation in the planar fabric. Additional shear zones are present trough out the study area but of significantly less magnitude resulting in three measured shear zones (Figure 17).

LV25004 6342154/532987

This additional shear zone is present in the same old granitoid, striking 84° and dipping 75° east. It has a slightly lesser width of 1 m but clear orientation across the exposure with same textural mineral alignment (Figure 7).

Figure 7. *Shear zone at outcrop LV25004 with well-defined structural alignment of minerals, compass for scale, 10 cm.*

LV25017 **Multiple deformation phases** 6342601/533214

First (1) and oldest of the three is a layered strongly deformed wavy rock, consisting of quartz 50%, K-feldspar 20% and dark biotite or amphibole 30%. The deformation of this rock is striking 154° with a 75° dip westward. Second rock (2) is fine to medium crystalline with similar composition of quartz 50%, plagoclase10%, K-feldspar 20% and biotite/amphibole 20%. The deformation is unidirectional and clear, striking 109° with a dip of 84° east. Youngest (3) and the last deformation consists of a dark granite with the make up of quartz 40%, K-feldspar 25%, biotite, and dark minerals 35%. The rock is medium to almost coarse crystalline with deformation showing of a strike at 120° and dip 82° east (Figure 8).

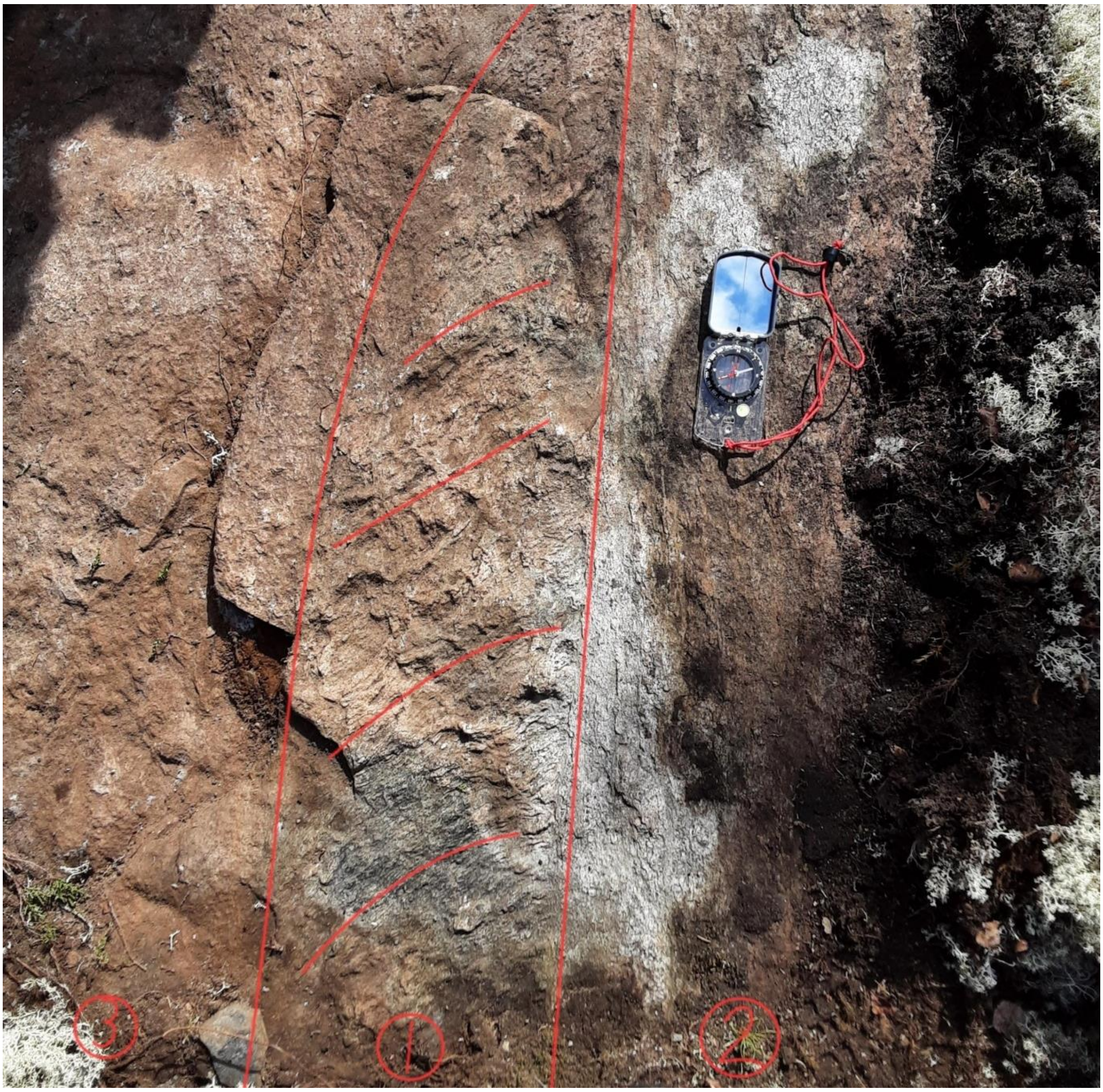

Figure 8. *Image of multiple deformations at LV25017 with highlighting annotations for clarity, compass for scale, 10 cm.*

LV25003 **Cutting fine crystalline pink granite** 6342176/532987

Several fine crystalline pink granite intrusions cut through old granitoid host rock. Ranging from 1 cm in width to over 30 cm they cut sharply as plains in an irregular network. There is no visible internal deformation of the homogenous pink granite. The best representation of this is the outcrop LV25003 Figure 9, but they are found trough out the the mapped area with varying sizes and recurrence.

Figure 9. *Cutting fine crystalline pink felsic intrusions in old granitoid LV25003, supervisor that indicate outcrop scale.*

LV25007 **Composite dike** 6342086/532361

Cutting through intermediate Växjö granite is a composite dike of gabbro and felsic composition. The dike is close to 2,5 m wide with dark green medium crystalline gabbro that appear on both sides of a central core with felsic composition. The felsic part consists of a light pink fine to medium crystalline mass with a slight porphyritic texture. The contact between the felsic and the gabbro is sharp but not planar at one side, irregular with a more faded contact at the other and there are no strong tendencies to mix or interact visible (Figure 10).

Figure 10. *Composite intrusion with felsic light pink core bordered by dark green mafic material LV25007. The contact is irregular but sharp with no visible mixing, geological hammer for scale, ca 50 cm.*

LV25055 **Felsic fractures in gabbro** 6342573/532377

The outcrop is a gabbroic dike that is 15m to 20 m wide and 100+ m long, with a dark green homogenous medium crystalline size. The dike is found cutting trough the fine crystalline pink Växjö granite. At weathered surfaces, a strong ophitic texture is seen and displays the mineral plagioclase and pyroxene/amphibole. Fractures of white felsic composition that ranges from 1cm to 10 cm wide intrudes the gabbroic outcrop in a sporadic non uniform pattern. The contact of the fractures is sharp but irregular (Figure 11). Within the white felsic intrusion is small mafic mineral crystals also observed.

Figure 11. *Sharp irregular contact between felsic intrusions and gabbro host rock LV25055, geological hammer for scale, ca 50 cm.*

LV25052 **Brecciation of gabbro** 6342836/532332

A gabbroic 5m wide dike is observed intruded upon, located within a fine crystalline granitic anatectic melt rock body. The contact with the fine gabbro and the felsic rock is sharp but irregular and the gabbro appears brecciated. The angular to sub angular gabbroic fragments are enclosed by the felsic matrix and distributed unevenly along the contact zone, illustrated for visual context (Figure 12b). With varying sizes spanning between 5cm to 20 cm the gabbroic clasts show slightly softened edges, and their color has transitioned from dark green to a lighter shade (Figure 12). The felsic rock flowing around the clasts is not homogenous and varies in color, composition, and crystal size. The color changes from light pink to orange with a dark gray tint. The composition mirrors the exhibiting color, going from felsic fine crystalline granitic to a gabbroic altered hybrid, which has crystallized as fine to slightly over medium crystalline orange and dark green minerals.

Figure 12. *Angular fragments of dark green gabbro enclosed within light pink fine crystalline felsic matrix at LV25052, compass for scale, 10 cm.*

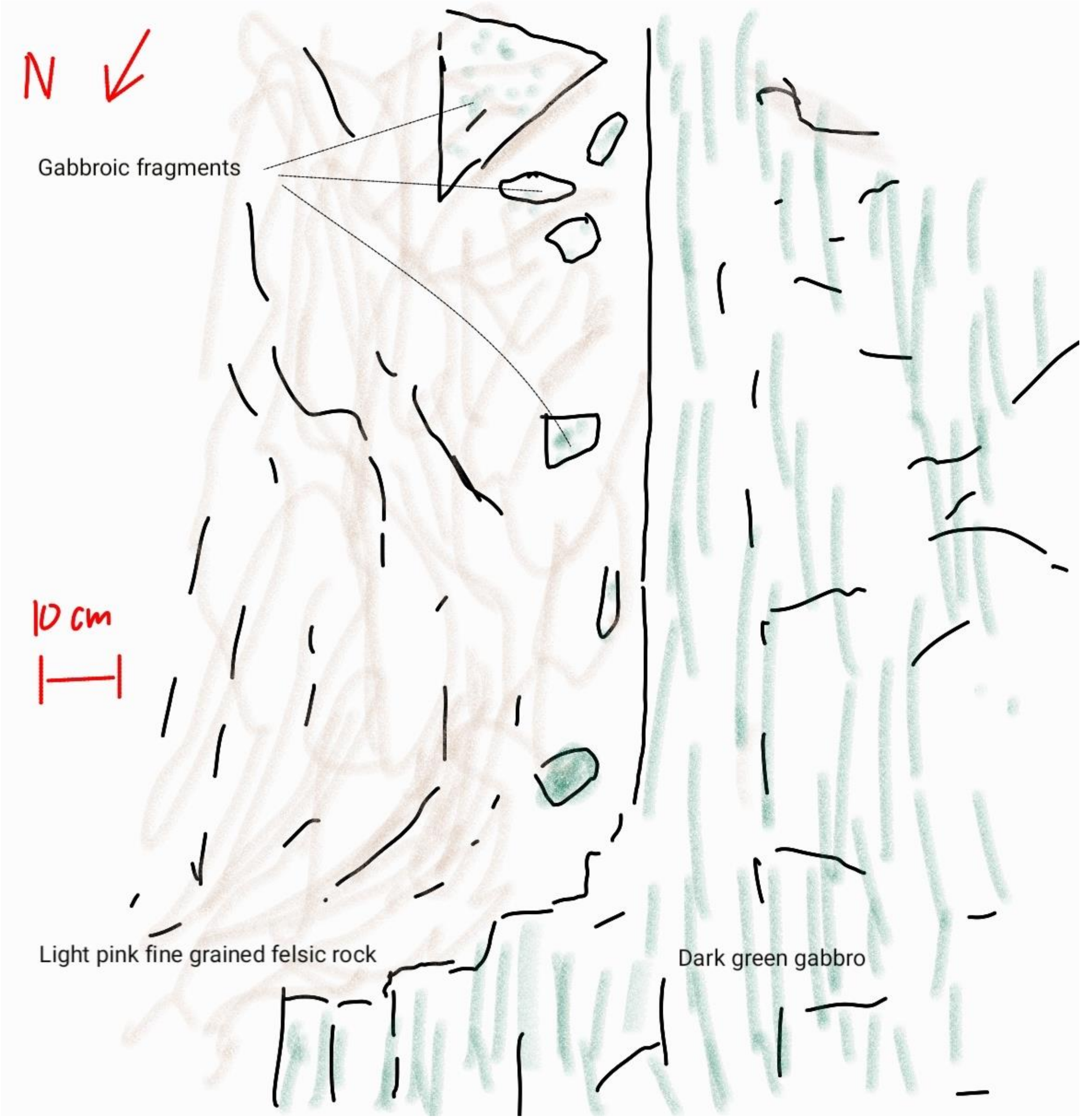

Figure 12b. *Illustrative sketch of outcrop LV25052 highlighting the clasts of dark green gabbro enclosed within light pink fine crystalline felsic matrix.*

LV25029 **Compositional variation within the granite** 6342867/532714

Surrounded by fine crystalline pink granite, this outcrop is compositionally different. A close inspection revealed three various compositions, one inhomogeneous light pink with mafic elements that varies strongly in crystal size from fine to coarse. The color is mainly light pink but transitions to a whiter tone where more quartz is present, or a darker gray to greenish color at places where mafic material is part of its matrix. In the outcrop its found as a fluid intrusion structure, creating a network around and in fractures trough the other two rock compositions.

The second rock is mafic with dark spots, medium crystalline to slightly above with a composition of plagioclase and pyroxene or amphibole. This composition is found as sub rounded to angular fragments that varies from 4 cm up to 40 cm in size. The fragments are fractured with the felsic light pink rock around and in the fractures. Last of the three is a mafic composition that is fine crystalline with green color, where minerals amphibole or epidote is present. Structurally this composition is stretched out as elongated bands 2 cm to 5 cm wide, that flow in the main deformation's direction, illustration, and picture for context (Figure 13 / 13b). Deformation is measured after the parallel mineral layering with a strike of 52° and dip 86° east.

Figure 13. *Picture showing three rock compositions at outcrop LV25029 within fine crystalline intermediate anatectic melt, geological hammer for scale, ca 15 cm.*

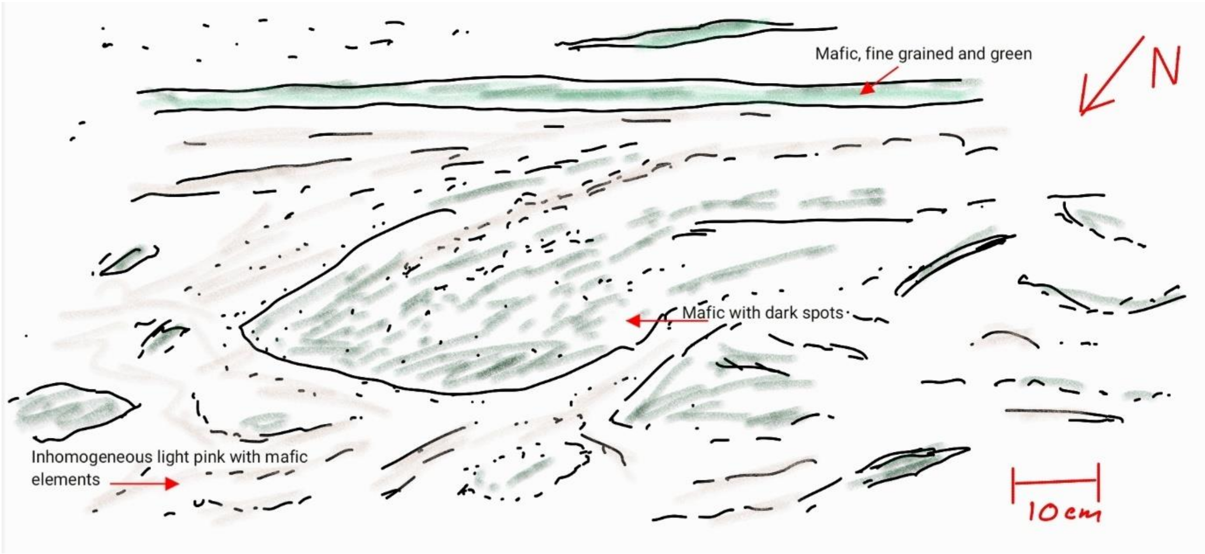

Figure 13b. *Highlighting sketch of three rock compositions in a outcrop within fine crystalline granitic anatectic melt LV25029.*

LV25060 **Heterogeneous rock assemblage** 6342473/532466

In a triple junction of gabbro, fine crystalline granitic anatectic melt LV25042 and the old granitoid LV25040, the representing outcrop is disordered. Banded fine crystalline felsic sections are followed by two different xenoliths varieties ranging between 2cm to 10cm in size. There are xenoliths of mafic dark green composition and xenoliths of felsic assemblage with structural banded wavy internal deformation. Surrounding the xenoliths are fine crystalline granitic anatectic melt and the old granitoid which partially merges in a ductile matrix texture (Figure 14).

Figure 14. *Heterogeneous rock assemblage LV25060 of a gabbro,* fine crystalline granitic anatectic melt *and the old granitoid, pencil for scale, ca 15 cm.*

LV25057 **Xenolith** 6342550/532315

Xenoliths were observed within the old granitoid (Figure 15). The xenoliths range in size from 2-3 cm up to 20 cm, their typical shape is sub rounded to a drawn-out elongated form. With a slightly deformed look and exhibiting a week foliation they are distributed in no coherent fashion. They are fine to medium crystalline with a sub porphyritic texture, darker gray with a pinkish undertone in color and exhibit a slightly diffuse but visible contact with the host granite.

Figure 15. *Xenolith within old granitoid LV25057 showing sub rounded shape, pencil for scale, ca 15 cm.*

3.1.3 Mapped Results from the Study Area

Results from petrographic interpretations and field mapping is compiled into two maps that represents the geological outcrops of approximate shape, geology, and structural features.

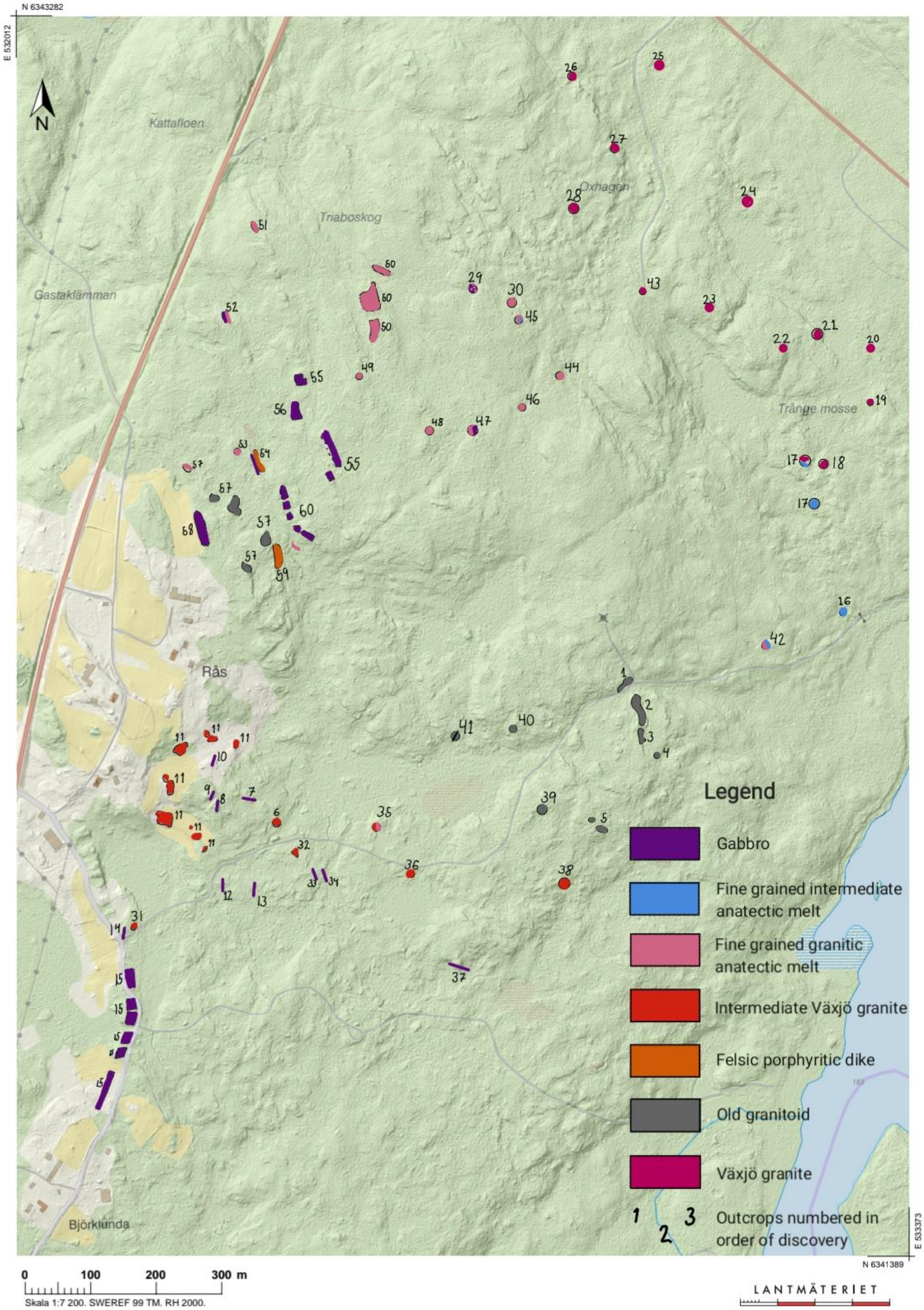

Figure 16. *Field based mapping results, with the locations and the outcrops approximate shape and geology numbered in order of discovery (1-60). Modified from elevation and base map. Source:(Min Karta, n.d.).*

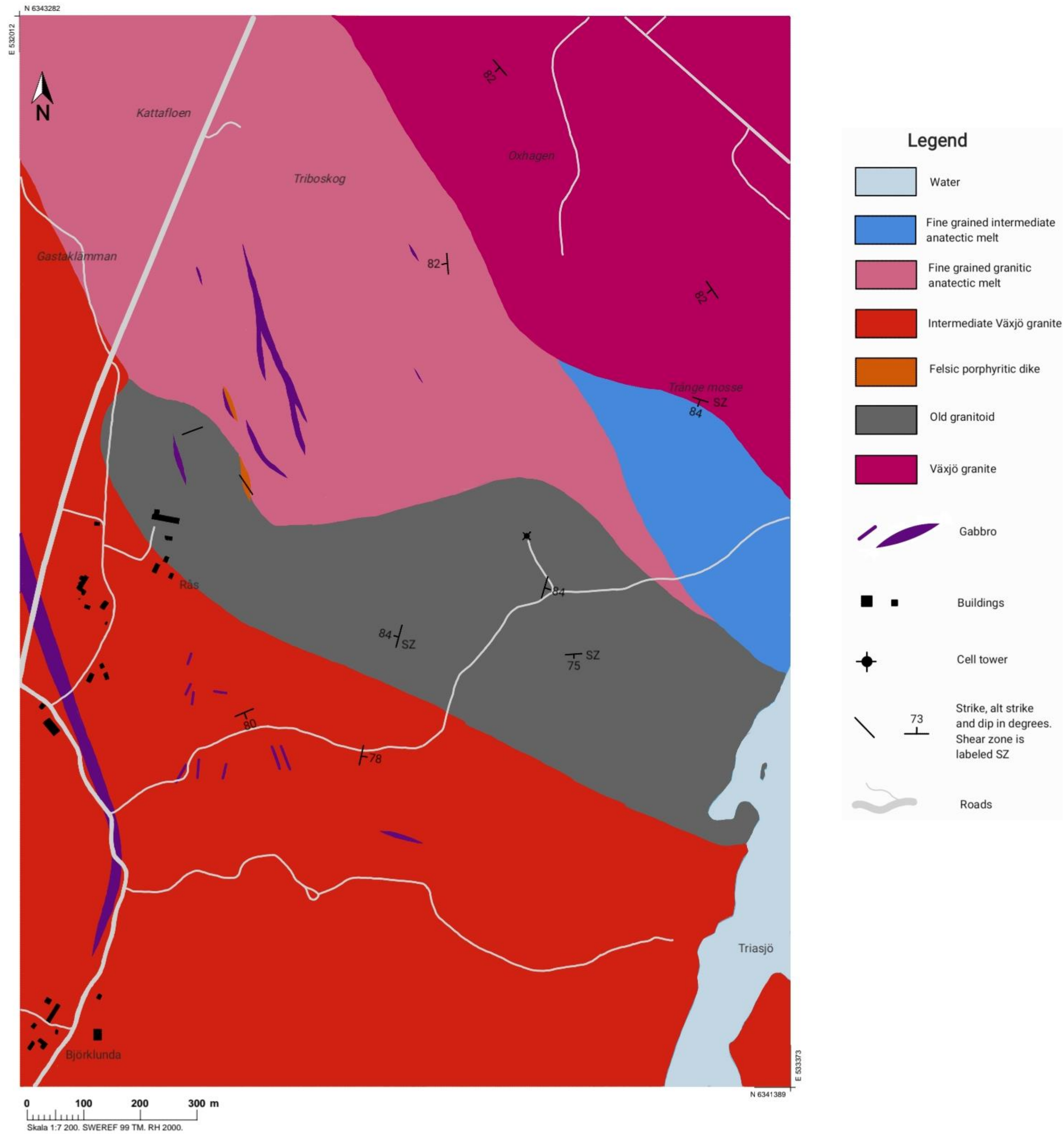

Figure 17. *Interpreted geological map over the study area, based on field observations, petrographic thin section analysis and spatial relationships among the units. The map represents a conceptual distribution of lithological domains, a sparse set of shear zones and foliation directions.*

3.2 Petrographic Analysis

Furthered analysis of the study areas lithologies consists of petrographic observations. Rock samples collected in the field were made into thin sections, which allowed a more detailed examination of mineral composition, deformation and alteration or deformation relationships. Prior the thin section analysis suseptibilit and density measurements of different rock samples were made.

Figure 18. *Overview of rock samples and cut pre thin section cuboids as 4×2cm rectangles.*

3.2.1 Thin Section Descriptions

A total of 14 thin sections were analyzed as part of the study. All are included below for completness, particular emphasis is placed on samples LV25040, LV25016, LV25007A,LV25052A and LV25060. These are marked with (Key Sample) and represents key lithologies for interpeting their relationships to OJB and SVB. The remaining samples are included for comparison and documentation.

LV25040 **Old granitoid** **(Key Sample)** 6342209/532773

Table 1. Magnetic susceptibility, density, and modal mineral estimation of sample LV25040.

Magnetic susceptibility	3000-3500
Density	2,739 g/cm^3
Mineral	Modal estimation
Plagioclase	~ 40%
K-feldspar	~ 20%
Quartz	~ 15%
Biotite	~ 10%
Amphibole, Hornblende	~ 10%
Titanite	~ 2%
Sericite	~ 1%
Epidote	~ < 1%
Zircon	~ < 1%
Opaque	~ < 1%

This thin section is a medium to coarse crystalline sample with an inequigranular texture. Large crystals of plagioclase show signs of a disequilibrium state with embayment's, irregular crystal boundaries and sericitization. Anhedral smaller quartz crystals have crystallized around the plagioclase and K- feldspar. Myrmekitic texture is seen at K-feldspar boundaries, present within the crystals is sericite and additional exsolution lamellae. Seen as green brownish biotite in PPL with zircons burning circular haloes, the biotite shows deformation signs in the form of kink bands and a slight alignment of mineral crystals. Almost always accompanying the biotite are anhedral medium size hornblende crystals with opaques and subhedral to euhedral titanite (Figure 19). This puts the composition of the rock as a granodiorite.

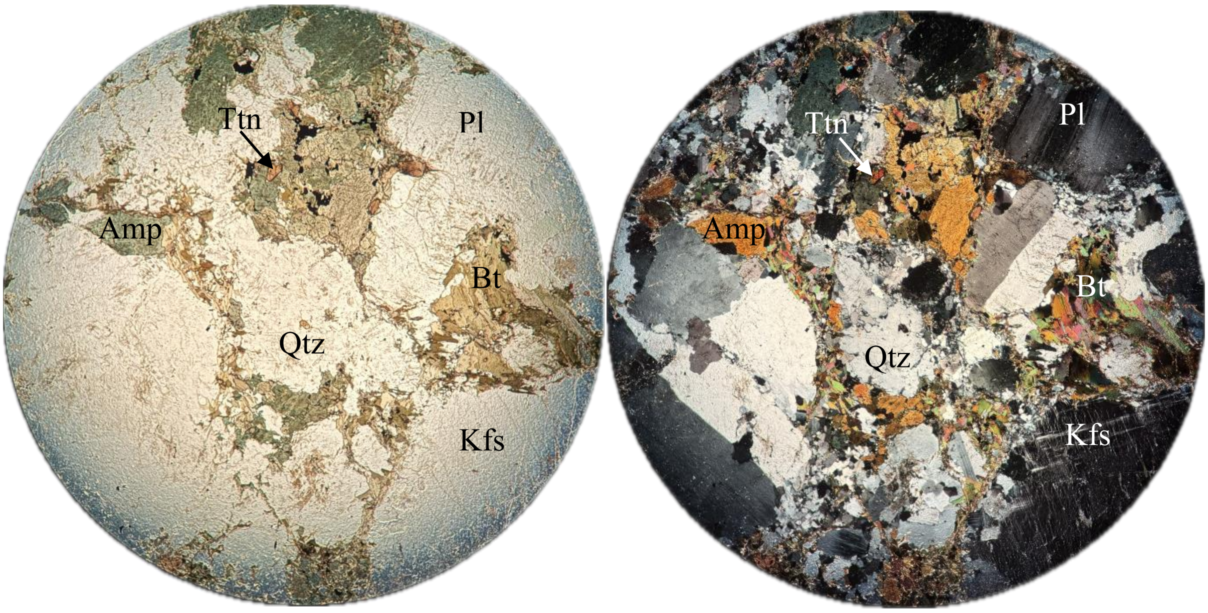

Figure 19. *Pictures of thin section LV25040 in 2,5x zoom, PPL to the left XPL to the right, visible field covers ~1cm.*

LV25042 **Fine crystalline granitic anatectic melt** 6342322/533158

Table 2. Magnetic susceptibility, density, and modal mineral estimation of sample LV25042.

Magnetic susceptibility	1500
Density	2,646 g/cm^3
Mineral	Modal estimation
Quartz	~ 45%
Plagioclase	~ 30%
K-feldspar	~ 10%
Opaque	~ 4%
Muscovite	~ 3%
Amphibole	~ 3%
Epidote	~ 2%
Biotite	~ 2%
Pyroxene	~ 1%

The rock in thin section exhibits alteration and hydrothermal overprint in a fine to medium crystalline make up, crystal boundaries are irregular, and the overall texture is inequigranular. Quartz shows lineation with anhedral slightly drawn-out crystals in a general direction. As slightly larger crystals surrounded by the quartz, plagioclase crystals with diffuse crystal boundaries exhibiting poikilitic texture. The incorporated crystals range from epidote, pyroxene, muscovite to amphibole, all very fine crystalline with a subhedral to euhedral shape. Biotite and the opaques both display foliation with a unidirectional deformation, biotite with the alignment of the platy mineral shape and the opaques in alignment along the same linear axis (Figure 20). The composition of this rock plots in the tonalite field.

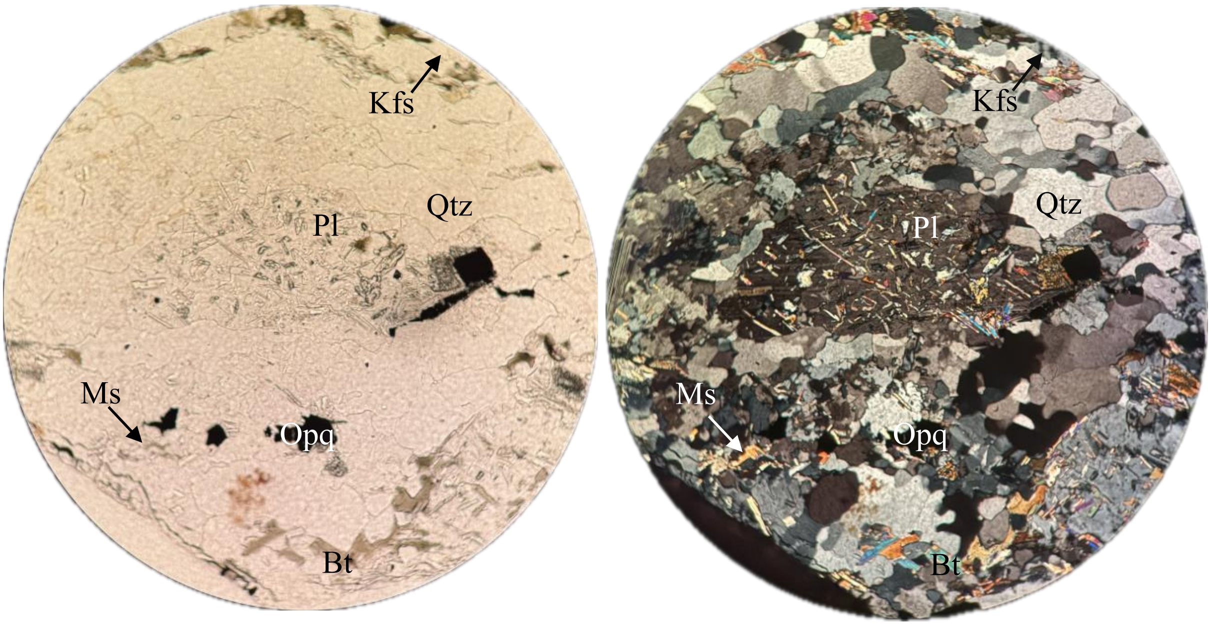

Figure 20. *Pictures of thin section LV25042 in 10x zoom, PPL to the left XPL to the right, visible field covers ~2mm.*

LV25015B **Fine Crystalline Gabbro** 6341811/532187

Table 3. Magnetic susceptibility, density, and modal mineral estimation of sample LV25015B.

Magnetic susceptibility	2000-3000
Density	2,980 g/cm^3
Mineral	Modal estimation
Amphibole	~ 35%
Plagioclase	~ 35%
Chlorite	~ 10%
Sericite	~ 5%
Pyroxene	~ 1%
K-feldspar	~ <1%
Quartz	~ <1%
Biotite	~ <1%

Exhibiting fine crystalline subhedral to anhedral crystals, which boundaries are irregular but form a poikilitic texture. The subhedral crystals of plagioclase show alterations to sericite and are enclosed by altered pyroxene. The alteration is seen in PPL as a green halo of fine flaky crystals of amphibole, chlorite, and sericite. Present opaques with accompanied biotite are distributed irregularly displaying no structural deformation (Figure 21). The percentages of the minerals place the composition as an amphibolite, naming it as an amphibole rich gabbro.

Figure 21. *Pictures of thin section LV25015B in 10x zoom, PPL to the left XPL to the right, visible field covers ~2mm.*

LV25015A **Medium to coarse Gabbro** 6341811/532187

Table 4. Magnetic susceptibility, density, and modal mineral estimation of sample LV25015A.

Magnetic susceptibility	30 000-40 000
Density	2,942 g/cm^3
Mineral	Modal estimation
Plagioclase	~ 50%
Amphibole (actinolite or tremolite)	~ 20%
Pyroxene	~ 10%
Chlorite	~ 10%
Sericite	~ 5%
K-feldspar	~ 2%
Opaques	~ 2%
Quartz	~ <1%
Calcite	~ <1%
Biotite	~ <1

Strong poikilitic texture is visible in the medium to coarse crystalline almost equigranular rock composition. Euhedral to subhedral plagioclase crystal range with straight to embayed edges, include patchy and following fractures, alteration to sericite. Surrounding the plagioclase are subhedral crystals of pyroxene that is in disequilibrium, showing replacement in the form of altered to green halos of flaky chlorite or amphibole, cores of muscovite with sericitic texture and has scattered inclusions of opaque crystals. Minerals of K-feldspar, quartz, calcite, and additional opaques are dispersed unevenly throughout the rock. A slight structural deformation is present in a unidirectional form, visible with alignment of fractures within the mineral crystals (Figure 22). Classification of this rock lands on an altered amphibole bearing gabbro.

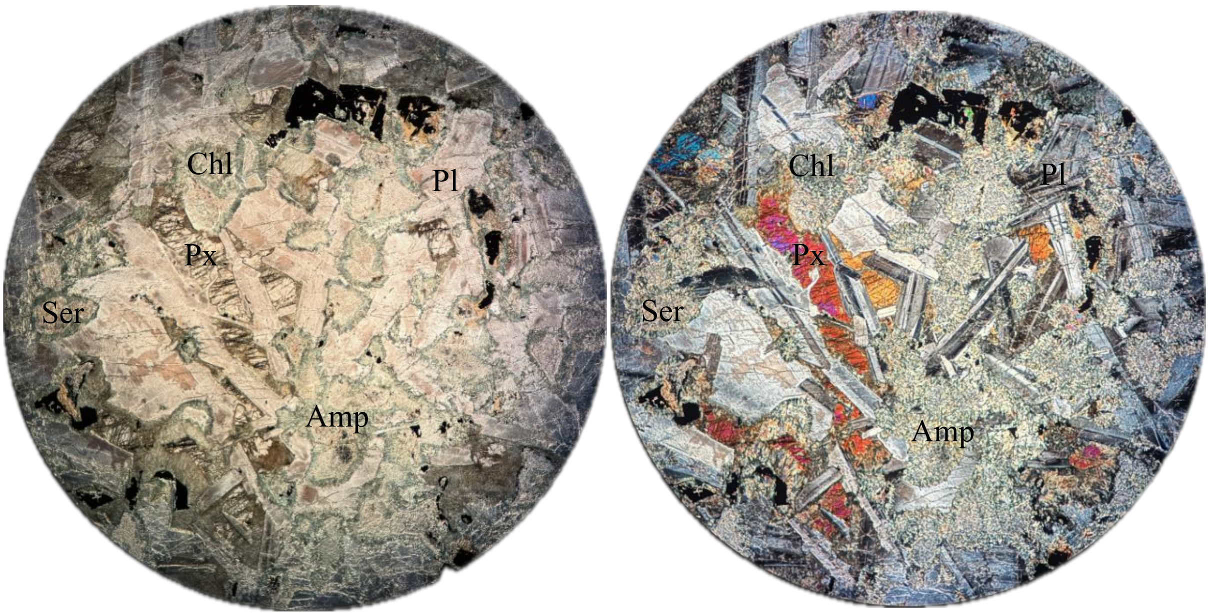

Figure 22. *Pictures of thin section LV25015A in 2,5x zoom, PPL to the left XPL to the right, visible field covers ~1cm.*

LV25016 **Fine crystalline intermediate anatectic melt (Key Sample)** 6342371/533271

Table 5. Magnetic susceptibility, density, and modal mineral estimation of sample LV25016.

Magnetic susceptibility	2000-8000
Mineral	Modal estimation
K-feldspar	~ 25%
Quartz	~ 25%
Plagioclase	~ 20%
Biotite	~ 15%
Opaques	~ 5%
Amphibole	~ <1%
Epidote	~ <1
Titanite	~ <1%
Zircon	~ <1%

Fine to medium crystalline sample with schlieren texture shown by streaking cluster bands of crystal accumulation. The schlieren represents zones composed primarily of fine crystalline opaques and biotite minerals, with addition of verry fine crystalline epidote, amphibole, titanite and zircon crystals. The remaining minerals display fine to medium crystal sizes, where anhedral plagioclase showcases patchy zones of K-feldspar replacement, sericitized and fine crystalline mineral inclusions. K-feldspar crystals of anhedral shape feature the same inclusion and sericite but with the addition of exsolution lamellae and myrmekitic replacement texture (Figure 23). Modal data points towards a granite in composition, with high mafic components.

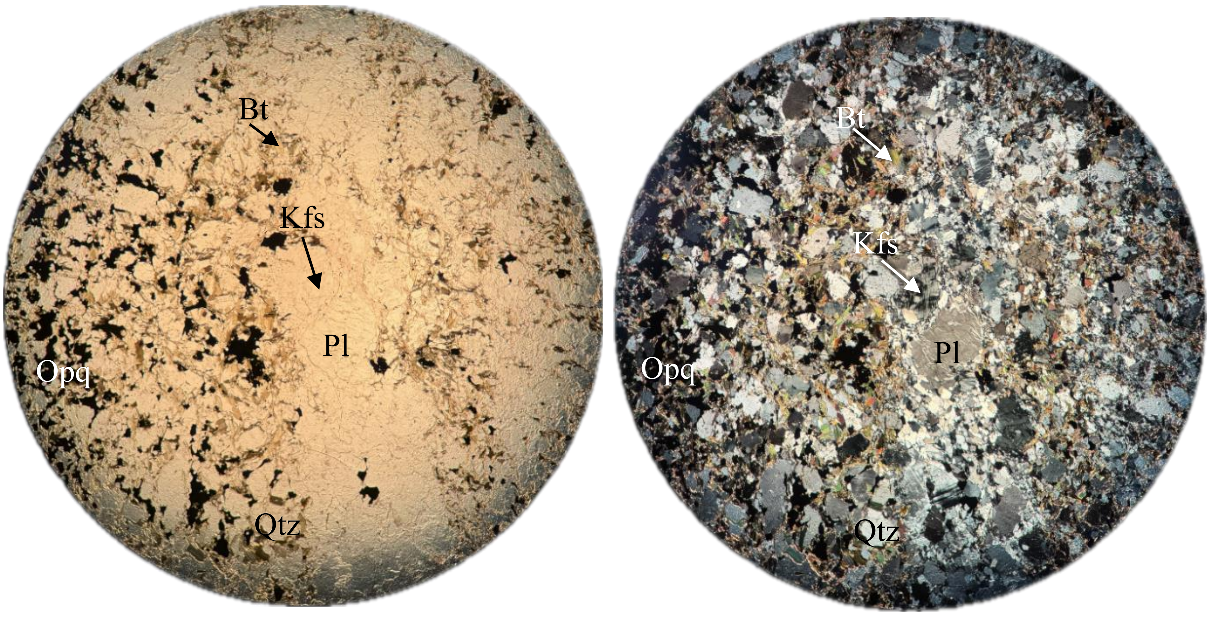

Figure 23. *Pictures of thin section LV25016 in 2,5x zoom, PPL to the left XPL to the right, both exhibiting schlieren texture streaking in a vertical direction, visible field covers ~1cm.*

LV25006 **Intermediate Växjö granite** 6342051/532403

Table 6. Magnetic susceptibility, density, and modal mineral estimation of sample LV25006.

Magnetic susceptibility	2000-8000
Density	2,694 g/cm^3
Mineral	Modal estimation
Plagioclase	~ 35%
Quartz	~ 25%
K-feldspar	~ 20%
Amphibole, Hornblende	~ 7%
Biotite	~ 6%
Sericite	~ 3%
Epidote	~ <1%
Opaques	~ <1%
Zircon	~ <1%

The crystalline minerals are subhedral showing slight foliation and with a variation from fine to coarse displaying a sub porphyritic texture. Phenocrysts of plagioclase show, sericitized embayed boundaries and inclusions of smaller other crystals. K-feldspar phenocrysts with disequilibrium textures exhibit exsolution lamellae and myrmekitic altered boundaries. Fine crystalline anhedral quartz gains enclose the plagioclase, K-feldspar, and present amphibole, distinct with their blue to green pleochroism and 120° 60° cleavages. Adjacent and often accompanying the amphibole is biotite with inclusions of zircons, small epidote crystals and opaques, these minerals have a slight tendency to align along a linear axis showing a slight liniated fabric (Figure 24). This sample is best classified as a granodiorite with its modal estimation.

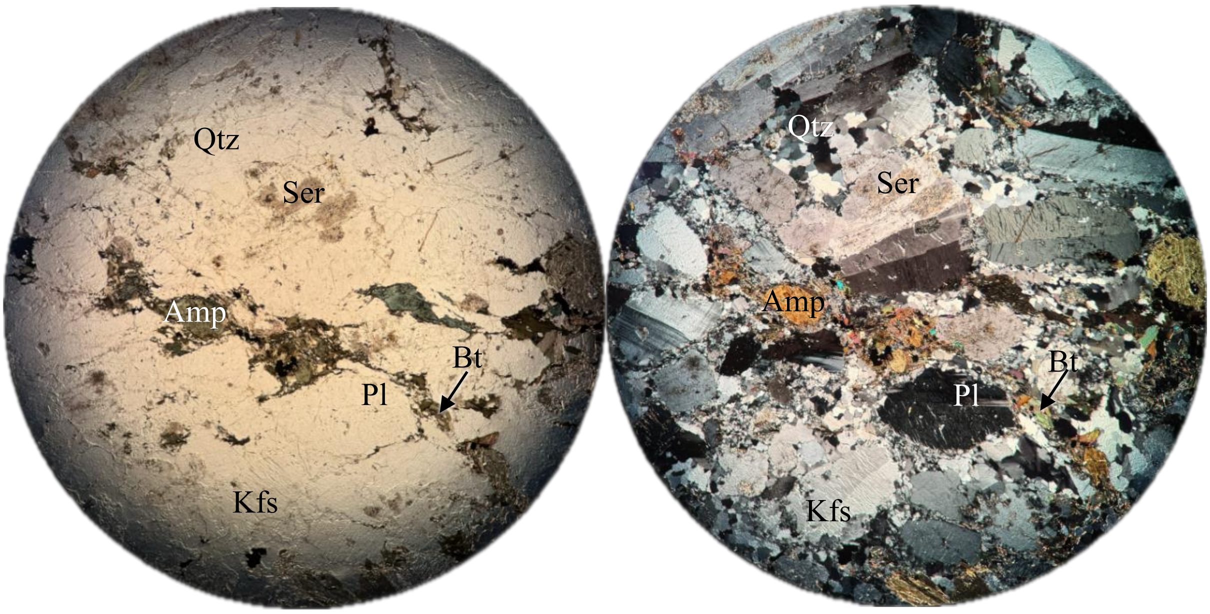

Figure 24. *Pictures of thin section LV25006 in 2,5x zoom, PPL to the left XPL to the right, visible field covers ~1cm.*

LV25054A **Porphyritic felsic dike** 6342603/532377

Table 7. Magnetic susceptibility, density, and modal mineral estimation of sample LV25054A.

Mineral	Modal estimation
K-feldspar	~50%
Quartz	~ 40%
Plagioclase	~ 7%
Biotite	~ 3%
Opaques	~ <1%
Epidote	~ <1%
Rutile	~ <1%
Sericite	~ <1%

Clear porphyritic texture with subhedral phenocrysts in anhedral verry fine crystal matrix (Figure 25). The make up of the phenocrysts are relict plagioclase replaced by Sericite and K-feldspar which show embayments at the boundaries, inclusions of other minerals and additional cracks filled in with matrix. The composition of the matrix is a mix of mainly quartz and K-feldspar, with a random distribution of biotite, opaques, epidote, and rutile crystals. Deformation is seen as slight unidirectional alignment of crystalline matrix. Classification of this rock land upon a porphyritic rhyolite dike.

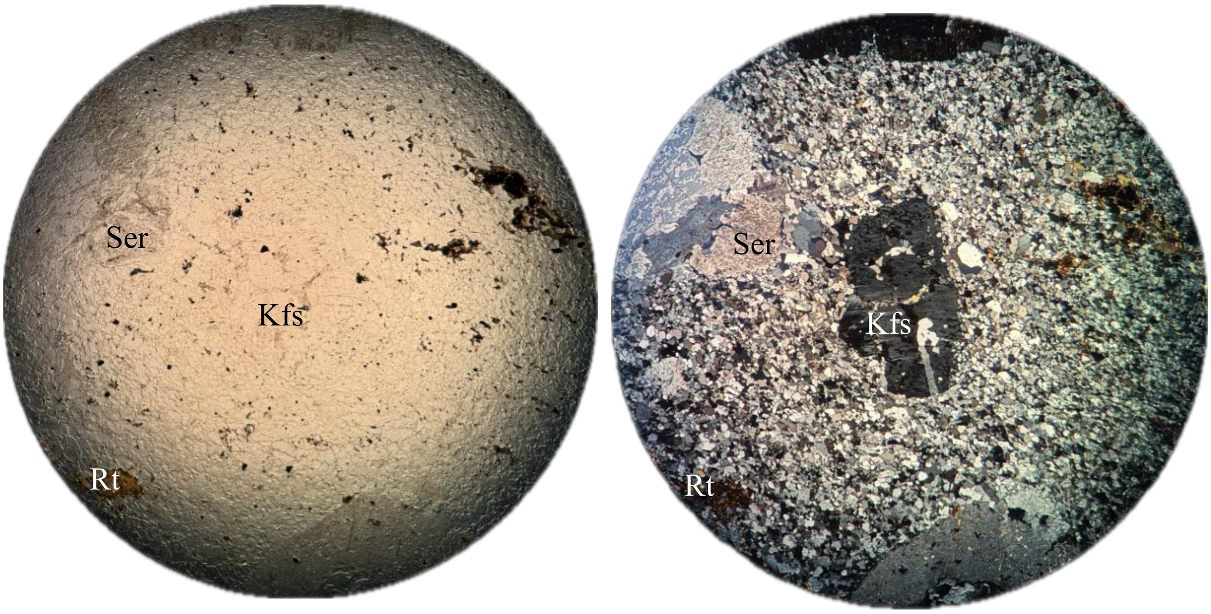

Figure 25. *Pictures of thin section LV25054A in 2,5x zoom, PPL to the left XPL to the right, visible field covers ~1cm.*

LV25041 **Shear zone in Old granitoid** 6342186/532682

Table 8. Magnetic susceptibility, density, and modal mineral estimation of sample LV25041.

Magnetic susceptibility	1500-2500
Density	2,745 g/cm^3
Mineral	Modal estimation
Quartz	~50%
Plagioclase	~20%
K- feldspar	~10%
Biotite	~7%
Amphibole, Hornblende	~5%
Epidote	~1%
Pyroxene	~ <1%
Rutile	~ <1%
Titanite	~ <1%
Zircon	~ <1%
Opaques	~ <1%

Inequigranular and foliated, showing preferred mineral orientation in the rock fabric (Figure 26). Deformed anhedral plagioclase is seen with embayments and inclusions. Amphibole is oriented along the strain axis together with small subhedral short prismatic pyroxene. Quartz is found with undulatory extinction as slightly elongated shaped crystals. Sericitization is present throughout the feldspar crystals, not sparing the anhedral K-feldspars that also display disequilibrium reactions with myrmekitic texture. Strong foliation is visible as biotite with zircon inclusions is in alignment, oriented in the same direction is rutile and enclosing around some opaque crystals. Nestled against these and following the unified directional trend is both anhedral titanite and epidote crystals. This places the rock as a sheared granitoid with strong foliation.

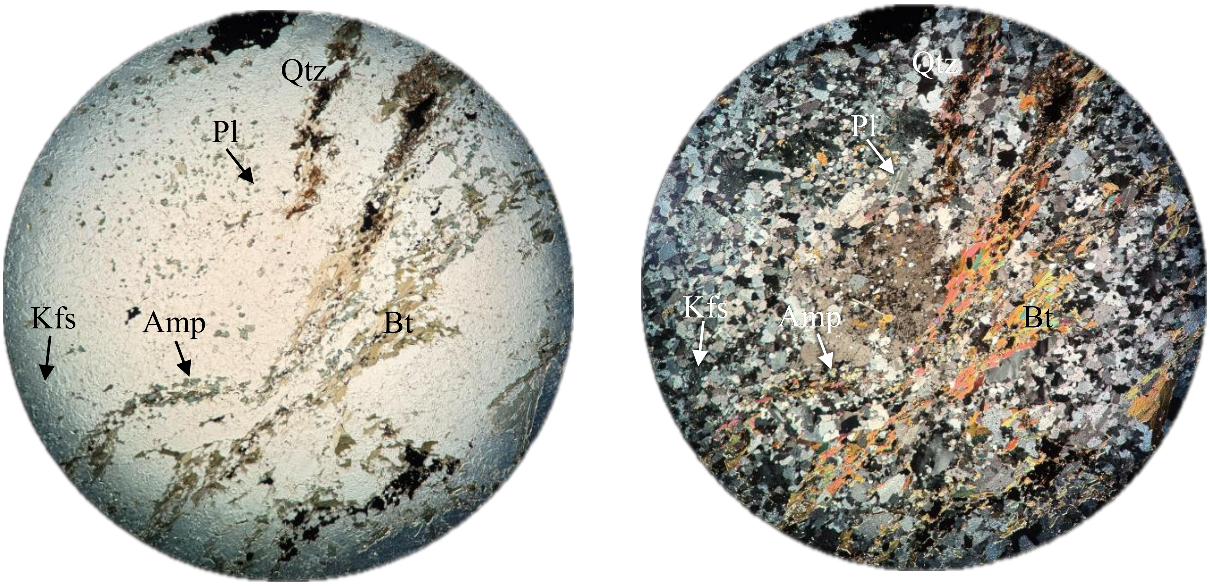

Figure 26. *Pictures of thin section LV25041 in 2,5x zoom, PPL to the left XPL to the right, visible field covers ~1cm.*

LV25017 **Multiple deformation phases, Youngest (3)** 6342601/533214

Table 9. Magnetic susceptibility, density, and modal mineral estimation of sample LV25017.

Magnetic susceptibility	3000
Mineral	Modal estimation
K-feldspar	~ 35%
Quartz	~ 30%
Amphibole, Hornblende	~ 15%
Plagioclase	~ 10%
Biotite	~ 3%
Epidote	~ 1%
Sericite	~ 1%
Rutile	~ <1%
Pyroxene	~ <1%
Opaques	~ <1%
Zircon	~ <1%

The thin section exhibits lineation with slight foliation within varying crystal sizes from fine to coarse. Quartz is seen with undulatory extinction and are elongated in parallel to the deformation strain axis. Anhedral sub phenocrysts of K-feldspar show perthitic texture with exsolution lamellae and intergrowth of myrmekite texture favouring replacement of quartz and plagioclase. Plagioclase crystals of anhedral character demonstrate features that all feldspar crystals in the sample show, internal inclusions and sericitization. The lineated slight foliation consists of aligned biotite with zircons, extended amphibole crystals with inclusions, pyroxene crystals with inclined extinction, anhedral finer crystals of epidote, rutile, titanite and lastly opaques (Figure 27). The final classification puts it as a deformed alkali feldspar granite displaying almost gneissic texture.

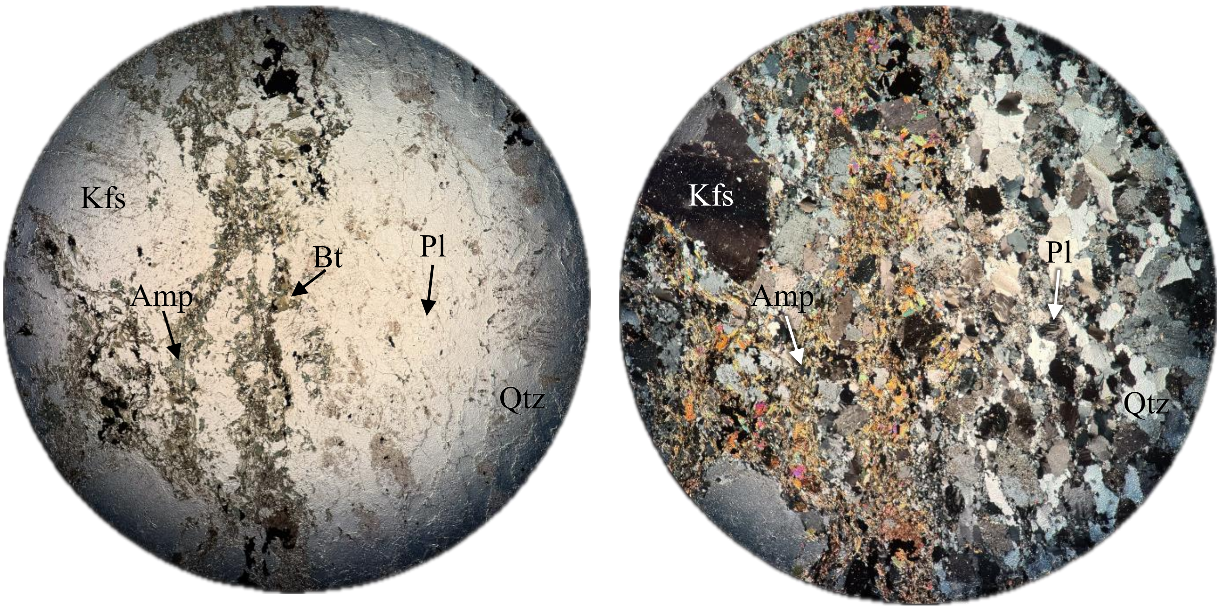

Figure 27. *Pictures of thin section LV25017 in 2,5x zoom, PPL to the left XPL to the right, visible field covers ~1cm.*

LV25007A **Composite dike, Felsic** **(Key Sample)** 6342086/532361

Table 10. Magnetic susceptibility, density, modal mineral estimation of sample LV25007A.

Magnetic susceptibility	1000-2000
Density	2,615 g/cm^3
Mineral	Modal estimation
Quartz	~ 45%
K-feldspar	~ 30%
Plagioclase	~ 15%
Biotite	~ 1%
Opaques	~ 1%
Rutile	~ 1%
Epidote	~ <1%
Titanite	~ <1%
Amphibole, Hornblende	~ <1%
Sericite	~ <1%

Foliated sample with intergrowth texture in a fine crystalline matrix showing sub porphyritic tendencies. The matrix consists of mainly finer K-feldspar, plagioclase, and quartz, seen subhedral with a tendency to exhibit elongation in the direction of tectonic strain (Figure 28). Two different replacement processes are indicated by the replacement of subhedral plagioclase phenocrysts by K-feldspar that show patchy like appearance. Vermicular quartz intergrowth, displaying myrmekitic texture show the second replacement where K-feldspar is unstable and favours plagioclase and quartz replacement. Sericite is present and slightly replace the different feldspar crystals. Constituents of epidote, rutile, biotite, titanite and opaques are aligned in parallel with the foliation. Additionally, amphibole sporadically appear with an elongated prismatic habit. The composition of the rock brings the classification to a quartz rich alkali feldspar granite.

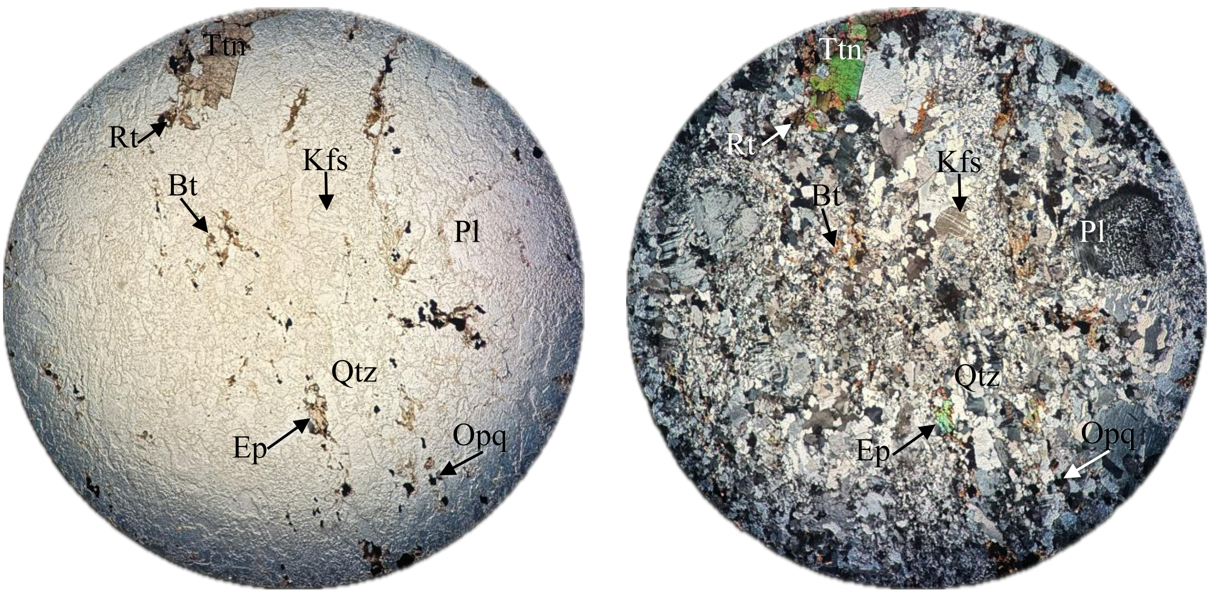

Figure 28. *Pictures of thin section LV25007A in 2,5x zoom, PPL to the left XPL to the right, visible field covers ~1cm.*

LV25007B Composite dike, Gabbroic 6342086/532361

Table 11. Magnetic susceptibility, density, modal mineral estimation of sample LV25007B.

Magnetic susceptibility	15 000-20 000
Density	2,971 g/cm^3
Mineral	Modal estimation
Plagioclase	~ 55%
Biotite	~ 10%
Olivine	~ 7%
Pyroxene	~ 5%
Chlorite	~ 5%
Amphibole	~ 5%
Opaques	~ 5%
K-feldspar	~ 5%
Quartz	~ 2%

Medium to almost coarse crystal sizes displaying strong replacement and sub ophitic texture (Figure 29). Subhedral plagioclase with a dirty and dusty appearance showcases sericitization, small mineral inclusions, fractures and disequilibrium textures demonstrated as resorbed diffuse crystal boundaries. Against the boundaries occurs anhedral quartz and K-feldspar patches. Relict crystals almost fully replaced are olivine, pyroxene, and amphiboles by biotite with the tendency to encapsulate opaque aggregates, chlorite, muscovite with sericitic texture, fine crystalline tabular amphibole microlites and some with elongate prismatic shape. Finalized as an altered biotite rich gabbro.

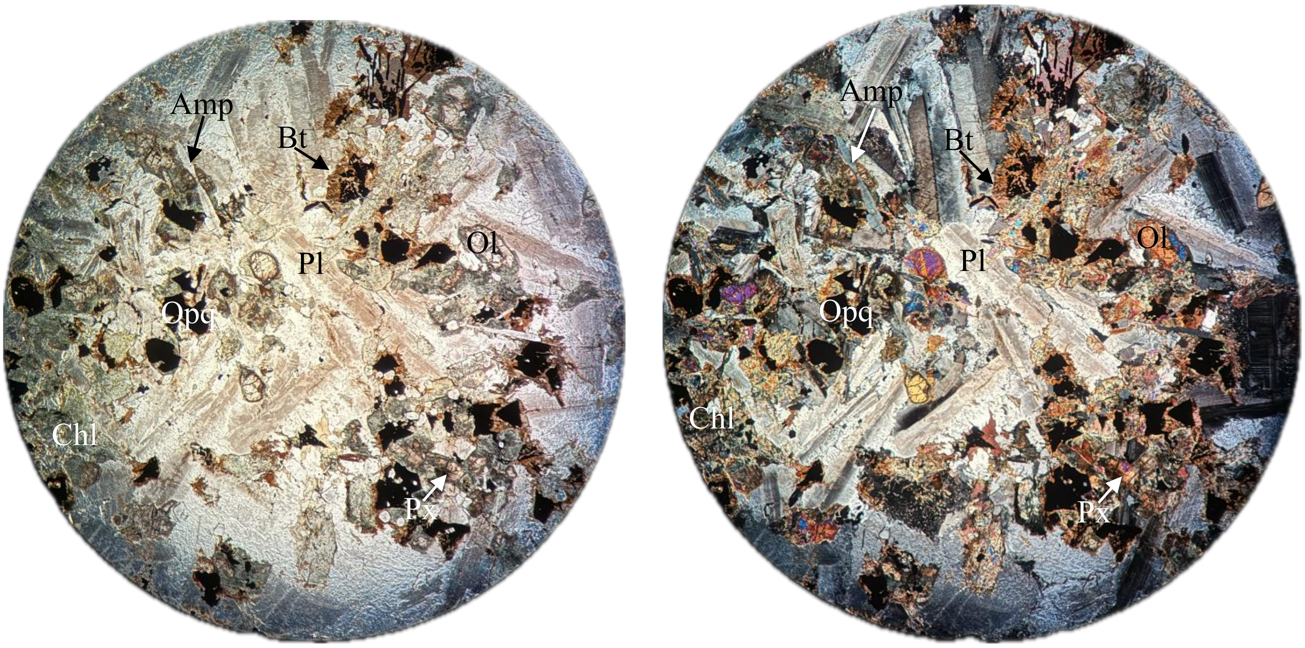

Figure 29. *Pictures of thin section LV25007B in 2,5x zoom, PPL to the left XPL to the right, visible field covers ~1cm.*

LV25052A **Brecciation of gabbro** **(Key Sample)** 6342836/532332

Table 12. Magnetic susceptibility, density, modal mineral estimation of sample LV25052A.

Magnetic susceptibility	400-1000
Mineral	Modal estimation
Plagioclase	~ 35%
K-feldspar	~ 25%
Amphibole	~ 20%
Chlorite	~ 15%
Pyroxene	~ 3%
Opaque	~ 2%
Epidote	~ <1

Fluid induced alteration of a medium to almost coarse crystalline sample with intergrowth texture. Subhedral plagioclase crystals show inclusions and disequilibrium with absorption around crystal boundaries. Amphibole display anhedral to subhedral shape with small opaques and other small mineral inclusions. Some amphibole crystals undergo chloritization and take the form of a foliated mylonitic chlorite fabric displaying kink bands and lens shaped relict amphibole, pyroxene, and epidote inclusions. Chlorite is also present in fractures and small inclusions inside the feldspar crystals as pervasive alteration Figure 30, the chlorites have a spherulitic radiating fan shape. Sporadically dispersed crystals of subhedral pyroxene and fractured opaques enclosed by epidote halos are also present. The sample is summarized as a chlorite altered amphibole bearing gabbro.

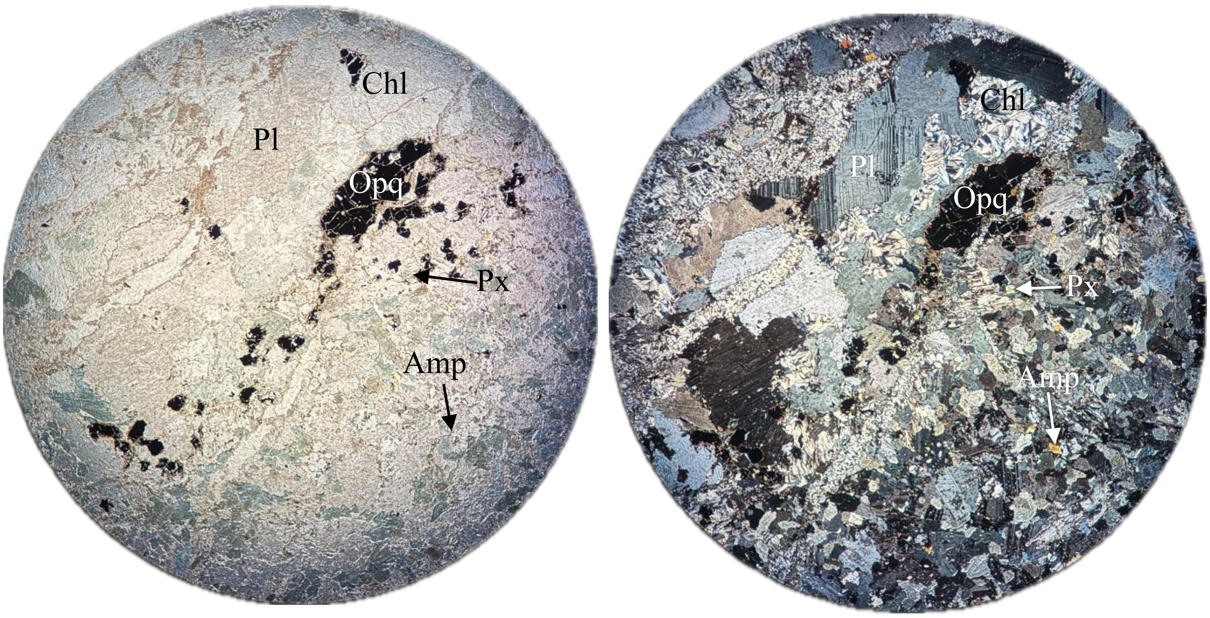

Figure 30. *Pictures of thin section LV25052A in 2,5x zoom, PPL to the left XPL to the right, visible field covers ~1cm.*

Table 13. Magnetic susceptibility, density, and modal mineral estimation of sample LV25029.

Magnetic susceptibility	1000-8000
Mineral	Modal estimation
K-feldspar	~ 35%
Amphibole, Hornblende	~ 20%
Plagioclase	~ 15%
Quartz	~ 15%
Biotite	~ 10%
Sericite	~ 2%
Epidote	~ 1%
Titanite	~ 1%
Opaques	~ 1%
Calcite	~ <1%
Rutile	~ <1%
Zircon	~ <1%

The coarse section of the sample displays a felsic dominated composition and the fine to medium crystalline section exhibit more mafic make up (Figure 31). Larger mineral crystals in the inequigranular sample consists of subhedral and sericitized K-feldspar, plagioclase alongside quartz with undulose extinction. Myrmekite is present, pointing toward disequilibrium and replacement. Biotite with zircons appear in proximity to amphibole, irregular anhedral amphibole clusters incorporate additional small epidote, titanite and opaque crystals with sporadic occurrence of rutile and calcite. Classification finalized as a compositionally heterogeneous granite with amphibole and biotite enrichment.

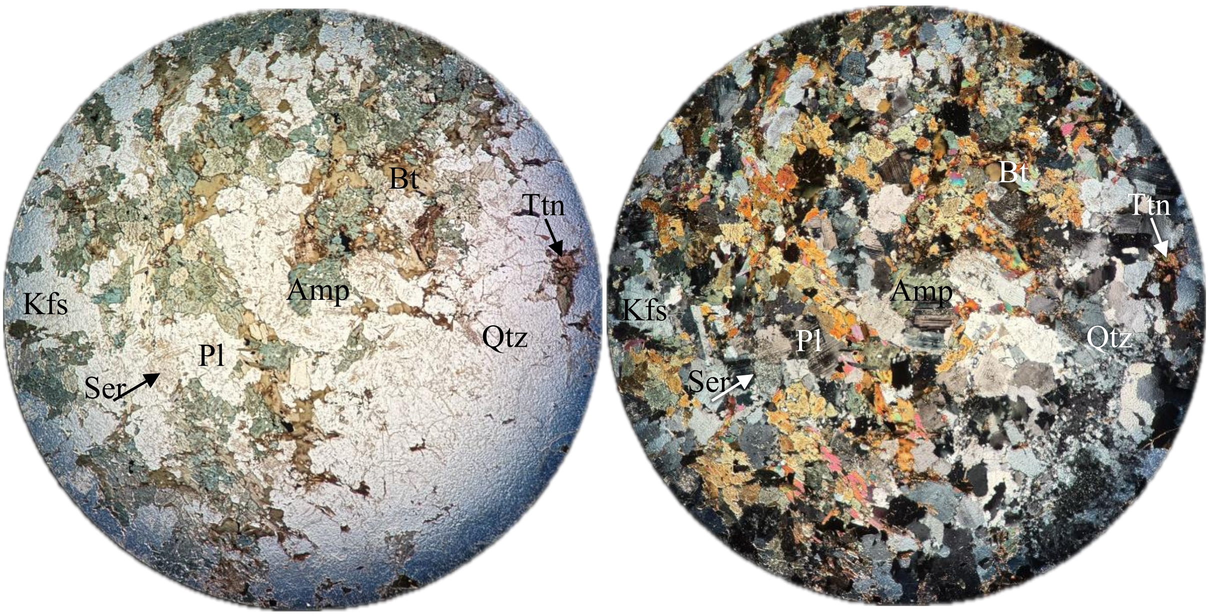

Figure 31. *Pictures of thin section LV25029 in 2,5x zoom, PPL to the left XPL to the right, visible field covers ~1cm.*

LV25060 **Heterogeneous rock assemblage (Key Sample)** 6342473/532466

Table 14. Magnetic susceptibility, density, and modal mineral estimation of sample LV25060.

Mineral	Modal estimation
K-feldspar	~ 30%
Quartz	~ 25%
Amphibole	~ 20%
Plagioclase	~ 15%
Epidote	~ 5%
Opaques	~ 2%
Titanite	~ 1%
Sericite	~ <1%
Chlorite	~ <1%

Inequigranular textured thin section with a centre of mafic fine crystalline constituents and medium crystalline more felsic encompassing composition (Figure 32). The fine crystalline assemblage making up the mafic centre is amphibole as subhedral patches with inclusions and other more prismatic crystals. Also present are anhedral quartz, plagioclase, epidote, titanite and discontinuous areas with chlorite and sericite. The fine crystalline centre has a transitional boundary of both crystal size and composition, going toward a larger ratio of slightly sericite feldspar. K- feldspar show exsolution lamellae and the boundary to adjacent plagioclase crystals, myrmekitic replacement occurs. Shapes are anhedral with replacement textures, inclusions, and quartz with undulose extinction is present at their boundaries. Same mafic components are observed with the larger crystals but more disperse, a localised faint tendency where opaque minerals emerging at higher interval with a slight concentration at the transitional boundary is also noted. This classifies the rock as a composite rock with mafic enclaves within a granitic host.

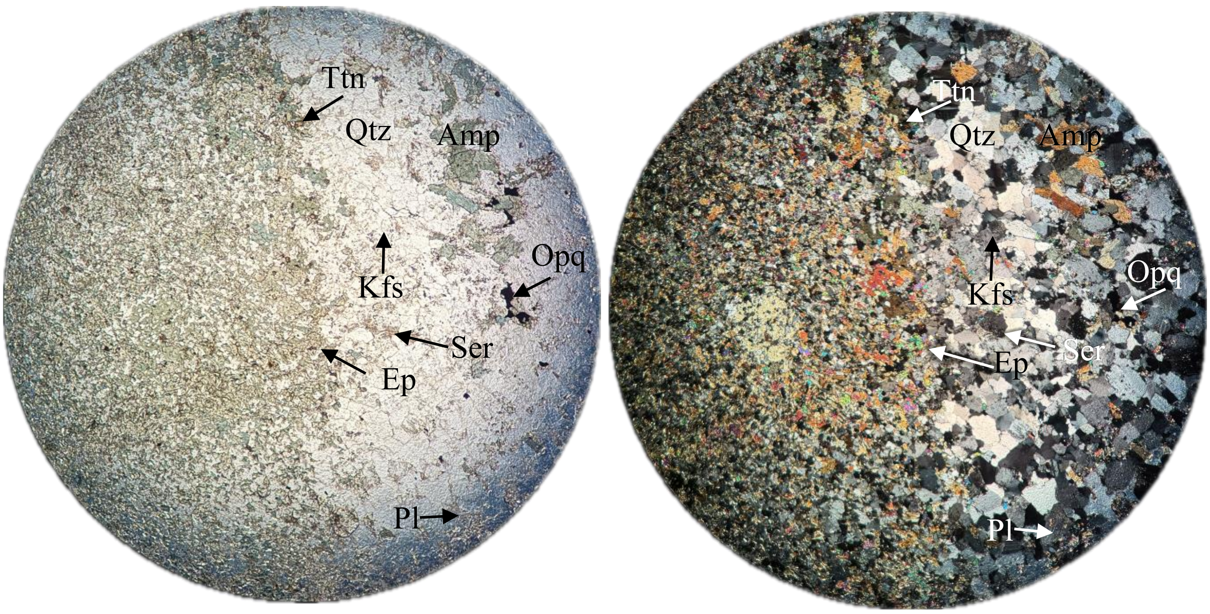

Figure 32. *Pictures of thin section LV25060 in 2,5x zoom, PPL to the left XPL to the right, visible field covers ~1cm.*

4. DISCUSSION

The following discussion aims to interpret findings made from observations and measurements taken from the field area near Virserum. These findings are evaluated in the form of geological relationships, deformation structures and lithological differences. The goal is to assess if there is support for the studied units to exhibit characteristics in line with OJB. The focus lies on deformation and metamorphism, whether the units are similar to surrounding SVB rock or have their own qualities.

4.1 Interpretations of Field and Structural Data

The main rock types observed are of granitic composition, with the old granitoid LV25040 located at the centre of the mapped area as an elongated profile in a NW and SE direction. Växjö granite LV25017 covers the northeastern part of the surveyed area. Betwen the old granitoid and Växjö granite, two lithologies consisting of a fine crystalline granitic anatectic melt LV25042 and fine crystalline intermediate anatectic melt LV25016 are determined to be located. To the west, an intermediate Växjö granite LV25006 covering the bottom part and the southwestern corner. The remaining lithologies consists of gabbro LV25015 and Felsic porphyritic dikes LV25054A intruding in a NW to SE direction.

Observed deformation covers different rock types and consists of a similar intensity and grade, Växjö granite, old granitoid and the intermediate Växjö granite display this similarity. In the Felsic porphyritic dike, a well pronounced strong foliation is present. Outliers with no clear foliation visible are the fine crystalline granitic anatectic melt, fine crystalline intermediate anatectic melt and the gabbro, indicating that they may intrude the crust at a later stage after the big deformation related to the Tönshult shear zone. This interpretation is supported by (Högdahl et al., 2004,section 2.5) who describe late stage mafic intrusions present in the region.

The crystal sizes of fine crystalline granitic anatectic melt, fine crystalline intermediate anatectic melt and gabbro show fine up to at most medium crystal sizes, indicating a quicker cooling. Comparably has Växjö granite, old granitoid and intermediate Växjö granite crystal sizes ranging from medium to coarse, indicating a longer and slower cooling rate. Excluded here is the felsic porphyritic dike, with phenocrysts that often relates to an initial phase of slow cooling during which the crystals could grow, followed by a stage of rapid cooling, forming the aphanitic matrix.

4.1.1 Boundaries and Unit Contacts

Observations of contact relationships in the field include crosscutting gabbroic dikes through the intermediate Växjö granite. A present cutting relationship between the Växjö granite in the NE corner and the fine crystalline intermediate anatectic melt, where the anatectic melt seems to cut the Växjö granite (Figure 8), supports the interpretation that the fine crystalline pink Växjö granite is intruding at a later stage.

Supporting this is the documented composite dike at locality LV25007 (Figure 10), where a gabbroic dike has a centre of felsic fine crystalline pink rock with strong similarities to the fine crystalline granitic anatectic melt. Further in line with the reasoning of a late-stage intrusive event is the presence of gabbroic dikes within the fine crystalline granitic anatectic melt, appearing without a crosscutting nature. Instead, the gabbros edges are diffuse and irregular, where melt interaction appears to absorb the gabbro. This places the gabbro as older than the fine crystalline granitic anatectic melt in relative age. The mafic, dark composition of the gabbroic dikes show signs of being incorporated into the fine crystalline granitic anatectic melt, changing the typical pink appearance to one more like an intermediate in composition. This is displayed as a transitional boundary between the two compositions.

In addition, fine crystalline pink felsic dike intrusions are documented at different outcrops, where the most pronounced display of this relationship is found within the old granitoid at outcrop LV25003 (Figure 9). There is relatively strong feasibility for in situ partial melting of adjacent rocks to occur at one such interaction, making the old granitoid a viable candidate to be the potential protolith of the anatectic melt. At rock outcrop LV25060 (Figure 14), the mingling and merging interaction of gabbro, old granitoid and a matrix strikingly similar to the anatectic melt further supports the reasoning that the old granitoid is a protolith candidate. Anatectic activity is linked to the SVB (Salin et al., 2021) leading support to the interpretation that the anatectic melt LV25016 observed in the field area formed during the crustal melting associated with SVB tectonism.

4.2 Geophysical Support from Density and Susceptibility

Comparing the gathered density and susceptibility measurements to the reference values in (Hrouda et al., 2009) the general trend for the granitic rocks in the study area indicates slightly higher density than typical, with readings around ~2,74 g/cm^3. Susceptibility readings ranged up to moderately high values of 4000-5000. Which adds support to the interpretation of hybridisation and mingling with gabbroic units.

The measurements of the gabbros exhibited density levels in the comparably medium to low range, approximately ~2,94-2,98 g/cm^3, whit susceptibility readings in the higher range, reaching up to 20 000-40 000. The lower density may be a result of visible chloritization, as observed in sample LV25052A (Figure 30), where chlorite appears to replace heavier minerals such as amphibole. This further supports the idea of fluid assisted mafic incorporation into the rock sample anatectic melt LV25016.

4.3 Petrographic Interpretation

From petrographic observations is the understanding over mineralogical composition, textures and deformation overprint gathered, with special focus on distinguishing features of OJB or SVB origin. Particular attention is given to key lithologies within the study area, specifically the old granitiod LV25040 and the anatectic melt LV25016.

4.3.1 Old Granitoid (LV25040)

The modal estimation of the old granitiod LV25040 Table.1 was plotted into a QAPF diagram and subsequently classified as granodiorite to tonalite in composition. Its assemblage contains a higher proportion of mafic minerals and is less potassium-rich than the more evolved SVB granites. In the study by Mansfeld et al.,(2005) describes the OJB to likely form as a continental margin volcanic arc with subduction related magmatism, marked by juvenile compositions. The comparatively more primitive mafic composition of the old granitoid LV25040, featuring abundant plagioclase, amphibole, and biotite, is consistent with the described arc derived melt of the OJB.

Xenoliths are observed in the old granitoid at outcrop LV25057 (Figure 15), they likely represent fragments of preexisting crust that were incorporated during ascent as an arc derived melt. This support the interpretation that the old granitoid is part of the Oskarshamn-Jönköping Belt (OJB).

The medium to coarse crystalline, inequigranular character suggests a slower cooling rate during intrusion. The arc system (which is the proposed magmatic system for the OJB) typically emplaces granitoids as plutonic bodies, indicating moderate to deep crustal levels. This implies slow to moderate cooling, resulting in a coarse crystalline rock, which aligns with the petrographic observations.

Exsolution lamellae in k-feldspar crystals are described in (Abart et al., 2009) to form below ~600°C in a sub solidus temperature range, where the rock has fully solidified but continues cooling changes the equilibrium to favour a new mineral structure, resulting in exsolution in the body of the crystal as lamellae. Such slow cooling is a defining feature of deep crustal plutonic environment.

Embayment in plagioclase with irregular crystal boundaries indicate disequilibrium, with a potential for partial resorption caused from changing magmatic conditions or later thermal overprint. The present sericitization of feldspars suggests alteration from hydrothermal activity, possibly linked to an SVB overprint during the post collisional orogenic setting (Andersson et al., 2006).

The myrmekite texture between plagioclase and K-feldspar crystals, support processes of migrating fluids. One indication of deformation after crystallization is biotite with kink bands, but the most suggestive evidence of deformation in the sample is the slight foliation and crystal alignment, which can be associated with SVB overprinting. As noted by (Rutanen, 2010) collisional orogenic belts such as the SVB have a tendency to rework older crustal blocks.

4.3.2 Anatectic Melt (LV25016)

Sample LV25016, referred to as a fine crystalline intermediate anatectic melt, displayed a granite composition when plotted in the QAPF diagram, but with a high proportion of mafic components. The finer crystalline matrix suggests moderate to rapid cooling, given the texture, it likely cooled in an intrusive dike setting. The texture is referred to as schlieren texture, consisting of streaking clusters of biotite and opaques that have accumulated through flow sorting, with no linear orientation, no platy minerals oriented in a strain direction and no extensional deformation of the opaques.

These structures reflect melt segregation and flow during partial melting. Their formation has been well documented in the (Milord & Sawyer, 2003) where schlieren texture are interpreted as evidence of melt mobility, indicating that the outcrop represents a intruding melt.
Accessory minerals such as amphibole, titanite, epidote and zircon are present as fine crystals within the schlieren streak accumulation. These are interpreted as protolithic crystals that survived due to higher melting point and were captured during melt flow, compositionally modified by mafic enrichment and incorporating from the most representative lithologies in the area, the old granitoid LV25040 and gabbroic dikes.

Signs of a complex alteration history in the anatectic melt are apparent, attributed to three coexisting replacement processes. First is replacement of plagioclase by K-feldspar, identified by patchy, vein like K-feldspar textures within relict plagioclase crystals. The second is seen as K-feldspar showing exsolution lamellae, implying the presence of crystals that experienced slow cooling, is present in a moderately fast cooling outcrop (Abart et al., 2009). The third alteration is replacement of K-feldspar by plagioclase, expressed through vermicular quartz forming a myrmekitic texture. The study by (Chakrabarty et al., 2024) points to fluid infiltration as the key process driving myrmekite formation.

The presence of sericite in feldspars provides further evidence of melt related alteration. Consistent felsic crustal melting is that temperatures needs to reach approximately ~ 650 °C to melt the rocks, in the absence of fluids (Wolf et al., 2018). However, the hydrothermal alteration features observed in the thin section anatectic melt LV25016, suggests fluid assisted melt generation, potentially lowering the melting temperature to around or slightly below 650°C.

These observations place the formation of the anatectic melt LV25016 within a crustal tectonothermal environment that was both hot and hydrous, likely tied to the SVB collisional magmatism and deformation, which is known to promote fluid infiltration and crustal reworking (Andersson et al., 2006).

4.3.3 Integration of Field and Petrographic Data

To further expand on the relationship between the old granitoid LV25040 and the anatectic melt LV25016, several supporting samples and field relationships are considered. Outcrop data from location LV25060 Figure 14 reveals three distinct components, of which old granitoid LV25040, the schlieren exhibiting anatectic melt LV25016 and the presence of mafic enclaves Figure 32 is observed together. The coexistence of these three compositions in the same outcrop points towards a genetic linkage, formed trough partial melting and hybridisation. Indicating melt interaction in the same geodynamic regime.

The composite dike at LV25007A/B provides additional context, consisting of both a felsic (A) and gabbroic (B) composition (Figure 10). The presence of both compositions suggests they where in a molten state simultaneously, enabling them to intrude together or in close succession. The felsic part (A) may represent a differentiated melt from the same magma chamber or a felsic anatectic melt. Its high quartz, K-feldspars content, along with low mafic mineral content, is indicative of an evolved felsic melt, likely derived from partial melting of crustal protoliths. A possible correlation exists between the felsic rock LV25007A and the anatectic melt LV25016. The mineralogical composition is similar, although LV25007A likely represents a more pristine felsic character. If it were to be subjected to conditions like those of the anatectic melt LV25016, it would be expected to exhibit the same features. Therefore, supporting the interpretation that the more pristine felsic LV25007A and the anatectic melt LV25016 represents the same melt type, expressed in different settings.

The anatectic melt is not homogenous in composition. The mineralogy and texture within the fine crystalline granitic anatectic melt LV25042 reflects this variability. A slightly lower mafic content in LV25042 likely represents less hybridisation during intrusion, suggesting the anatectic melt may have been derived from diverse sources and solidified before and full homogenisation occurred.

In the *Bergrundskarta Virserum* by Rontakokko and Mansfeld (2000), (excerpt of map at (Figure 3)), an Intermediate hybrid, dark/gray Växjö Granite a variant of the Växjö granitoid LV25006 is described, with centimetre wide dikes of a light red granite. This brings forward a possible event in which the anatectic melt LV25016 intrude the Intermediate Växjö granite LV25006, allowing plausible hybridisation.

Medium sized K-feldspar crystals with exsolution lamellae are present within the anatectic melt LV25016. As previously noted, this texture forms during slow cooling and prolonged sub solidus re-equilibration (Abart et al., 2009). Its presence in the moderately fast cooling outcrop anatectic melt LV25016, suggests that the crystals were incorporated from a slowly cooled, coarse crystalline felsic protolith.

Deformation described as foliation with preferred mineral orientation in the sheared old granitoid LV25041 Figure 26, provides evidence of a plausible SVB overprint. Given the sheared and fractured structure of the old granitoid LV25040 unit, which under the right conditions can act as pathways for melt to intrude, making the occurrence of partial melting a plausible interpreted scenario. Earlier observations by Rontakokko Mansfeld (2000) describe the granitoid unit in the study area as having undergone varying degrees of deformation and metamorphic overprint, including signs of magma mingling and assimilation. This supports the interpretation that the Old Granitoid LV25040 belongs to the OJB, was tectonically replaced into the SVB and subsequently overprinted melt thought to correspond with the dominant mineral assemblage in the anatectic melt LV25016. If anatectic melt generation is ongoing or remains mobile, it may migrate through these pathways and crystallize as veins and dikes. Outcrop LV25003 Figure 9 likely represents such an occurrence, positioning the old granitiod LV25040 as a plausible protolith candidate for the anatectic melt LV25016.

Further support for that the anatectic melt LV25016 remained mobile, comes from observations of gabbroic assimilation into the anatectic melt, documented at outcrop LV25055. This gabbroic outcrop is located inside the anatectic melt main unit, as seen comparing the map of outcrop locations Figure 16 to the interpreted geological map (Figure 17). It is recorded with felsic fractures cutting through it Figure 11 and the interpretations from the sharp and irregular contacts are that these fractures are anatectic melt injections, exploit brittle fractures in solidified gabbro.

A plausible further development of such interaction is seen at locality LV25052, where gabbroic clasts are separated from the host gabbro and incorporated into the anatectic melt (Figure 12/12b). Petrographic observations in thin section of the outcrop LV25052A show chlorite replacing amphibole, chlorite appearing as vein intrusions and small inclusions in feldspar crystals Figure 30, providing evidence for pervasive hydrothermal alteration. The gabbro has undergone both mechanical fragmentation and intense chemical/fluid alteration, defining the process as anatectic melt LV25016 assisted brecciation.

Interpretation of locality LV25029 describes an outcrop containing three compositions. The anatectic melt LV25016 intrudes a gabbroic body, resulting in subrounded mafic clasts surrounded by anatectic melt containing incorporated mafic elements and elongated green mafic bands (Figure 13/13b). Thin section analysis reveals diverse mineral assemblages, with coarse crystalline felsic domains (K-feldspar and quartz) adjacent to medium to fine crystalline zones rich in biotite and amphibole, as well as small epidote crystals (Figure31). Fluid induced alteration is evident through the presence of myrmekite disequilibrium textures and sericitization of feldspars. The presence of epidote supports the idea that hot fluids from the anatectic melt LV25016 caused partial melting or breakdown of amphibole, pyroxene, and plagioclase minerals in the gabbro. The result of this assimilation is reflected in the anatectic melts hybrid composition, visually captured in the schlieren texture of the anatectic melts sample LV25016 (Figure 23/5).

4.4 Synthesis: Tectonic and petrographic Evolution

The synthesis of field and petrographic observations leads to the following interpretations. The lithological unit represented by outcrop old granitoid LV25040, exhibits slow cooling under sub solidus conditions and has a granodioritic to tonalitic composition, is most appropriately interpreted as being of Oskarshamn-Jönköping belt (OJB) origin. Its mineralogical characteristics, low K-feldspar content, moderately higher density of 2,739g/cm^3 Table 1 and the occurrence of xenoliths Figure 15 (interpreted as fragments of incorporated preexisting crust) during its ascent as an OJB melt, all support this conclusion.

During collisional crustal thickening associated with the Småland-Värmlands belt (SVB), the old granitiod LV25040 was likely overprinted and partially melted. Additionally, the gabbroic component LV25007B of the composite dike is suggested to have acted as a thermal trigger for partial melting of the felsic crust, due to heat input from gabbroic intrusions.

The anatectic melt LV25016 is interpreted as being partially derived from the partial melting of the old granitoid LV25040. During the extrusion or movement of the melt, additional lithologies were incorporated into its composition, resulting in a hybridized melt. The identified schlieren texture of streaked clusters of biotite and opaques, serves as a strong indicator of melt flow. It is interpreted as a late-stage feature within the SVB, based on evidence of assimilation of late intruding gabbroic dikes in sample LV25052 Figure 12/12b and LV25029 (Figure 13/13b).

The heterogeneous rock assemblage at LV25060 Figure 14 provide crucial evidence of melt residue mingling, hybridisation and intrusion under conditions of ductile deformation. These features reinforce the model that an OJB derived protolith (old granitiod LV25040) was later reworked and remobilised during the thermal tectonic evolution of the SVB.

4.5 Limitations

The collected data exhibit some limitations, introducing uncertainties regarding the reliability of the measurements obtained. Deficiencies during the data compilation process occurred in several areas, particularly in field observations, where time constraints limited how densely measurements could be collected to cover a sufficient area for effective interpretation. Bedrock localities placed at ideal distances to fulfil this objective were not always accessible or identifiable. Moss and other overgrowth impeded visibility and a required temporary displacement, which further slowed down data collection, resulting in fewer overall data points. Not all measurements were consistently taken at each outcrop, some were missed due to human error, while others depended on the quality of the outcrop. Inconsistencies in the sampled data occurred due to misreading instruments or deprioritized calibration. To minimize this risk, multiple measurements was taken at each location, with the most representative values noted down.

The collection of rock samples for thin sections was depended on factors such as accessibility and the availability of suitable outcrop surfaces. Resistant surfaces with smooth texture proved difficult to sample, even with the use of a sledgehammer. Fractured and cracked zones were preferred, although the most representative location for a lithology was not always easily sampled. The collected rock samples reflect a balance between time constraints and the goal of

obtaining satisfactory material, resulting in variable sample qualities. However, no samples were taken haphazardly, sampling was undertaken carefully to maximize data quality.
Collected rock samples were used for density measurements, where accuracy was affected by human error, sample size and the precision of the weighing scale. Despite this, key parameters were met, and reliable data were obtained. Rock samples were cut into cuboids to produce thin sections, with the aim of presenting the best representation of the outcrop within a 4×2cm rectangle. Although careful attention was directed toward this objective, the reduction in scale from field outcrop size to thin section, inevitably results in a loss of geological resolution.

Time spent on thin section analysis was limited, resulting in a reduced scope of documented parameters. Priority was given to describing deformation textures and replacement features, leading to a narrower dataset. The quality of petrographic documentation is dependent on the observers experience and misidentification is plausible, particularly in highly altered samples or where small crystals with similar optical properties are present. Estimating mineral percentages by eye is inherently imprecise but deemed necessary to save time. When specific mineral identification could not be resolved, broader mineral group names were used. These limitations introduce a degree of uncertainty to the dataset.

The compilation of data into a geological map represents an interpretation of both field observations and thin section petrographic analysis. Uncertainties in the mapped contacts between geological units are inevitable, as the shapes and dimensions of subsurface features were extrapolated by connecting sparsely distributed outcrop data (Figure 16). Consequently, the highest resulting data reliability occurs closest to the observed outcrop localities. Lithological colors on the map should therefore be treated as a generalized summary of the field area, rather than a high-resolution geological model (Figure 17).

4.6 Recommendations for Future Work

Future work is recommended to help establish a stronger knowledge foundation, enabling clearer and more precise answers to the aim of this bachelor project. This includes data acquisition that contributes to a more detailed geochronology, particularly through isotopic dating focused on the old granitoid LV25040 and anatectic melt LV25016. This would help resolve the timing of intrusions, which would refine the intrusion sequence for easier interpretation. In addition, geochemical characterization of the study areas lithologies could better define lithological contacts, helping to distinguish transitional and sharp boundaries, thereby complementing, and refining the conclusions of the study.

5. CONCLUSION

The old granitoid LV25040 is characterized by abundant plagioclase, amphibole, and biotite, consistent with the juvenile arc magmatism associated with the Oskarshamn-Jönköping belt (OJB). During the collisional tectonism related to the Småland-Värmland belt (SVB), the old granitoid LV25040 was reworked, tectonically transported, and displaced within SVB units. SVB related magmatism introduced evolved granites, represented by the intermediate Växjö granite LV25006 and Växjö granite LV25018, bringing heat and fluids that may have initiate crustal anatexis. This thermal input likely induced partial melting of the OJB derived old granitoid LV25040.

The resulting anatectic melt, represented by samples LV25016 and LV25042, may have accumulated at depth and remained trapped for a period of time. Subsequently, gabbroic dikes, such as LV25015A/B, intruded the deformed SVB domain and the partially molten old granitoid LV25040, providing localized thermal input capable of inducing further melting. The anatectic melt LV25016 and LV25042 is therefore interpreted to be predominantly derived from the OJB old granitoid unit LV25040.

In later stages, the anatectic melt LV25016 and LV25042 underwent remobilization, intruding into gabbroic dikes or exploitable fractures. This process produced composite dikes like LV25007A/B, melt assisted intrusive breccias (LV25052) and hybrid rocks formed through mafic assimilation (LV25029 and LV25060). Ongoing melt movement caused alignment of assimilated mafic minerals, forming schlieren textures and displaying crosscutting intrusive relationships with neighbouring lithologies (LV25003). This melt crystallized to form rocks classified as anatectic melt LV25016 and LV25042, representing SVB related products with compositions influenced by both OJB derived old granitiod LV25040 and gabbroic components.
Taken together, the structural relationships, mineral assemblages and intrusive deformation features suggests that the studied rocks underwent a multistage evolution. Where inherited arc related OJB granitoids (Old granitoid LV25040) were recycled and experienced complex crust mantle interactions during later SVB post collisional tectonism, followed by thermal modification through mafic intrusions, ultimately giving rise to the hybrid anatectic melt LV25016.

6. ACKNOWLEDGEMENTS

I would like to thank my supervisor, Joakim Mansfeld, for his guidance and support. I also wish to thank Richard Gyllencreutz, for helpful input and assistance with logistics during the fieldwork.

Finally, I would like to express my gratitude to the Department of Geological Sciences at Stockholm University for providing resources and support throughout the project.

7. REFERENCES

Abart, R., Petrishcheva, E., Wirth, R., & Rhede, D. (2009). Exsolution by spinodal decomposition II: Perthite formation during slow cooling of anatexites from ngoronghoro, tanzania. *American Journal of Science*, *309*(6), Article 6. https://doi.org/10.2475/06.2009.02

Andersson, U. B., Eklund, O., Fröjdö, S., & Konopelko, D. (2006). 1.8 Ga magmatism in the Fennoscandian Shield; lateral variations in subcontinental mantle enrichment. *Lithos*, *86*(1–2), 110–136. https://doi.org/10.1016/j.lithos.2005.04.001

Chakrabarty, A., Karmakar, S., Dutta, U., Sanyal, S., & Sengupta, P. (2024). Evidence of fluid-induced myrmekite formation after alkali-feldspar megacrysts: An example from a meta-porphyritic granitoid in Makrohar, Madhya Pradesh, India. *Mineralogical Magazine*, *88*(3), 262–276. https://doi.org/10.1180/mgm.2023.90

Gorbatschev, R., & Bogdanova, S. (1993). Frontiers in the Baltic Shield. *Precambrian Research*, *64*(1), 3–21. https://doi.org/10.1016/0301-9268(93)90066-B

Högdahl, K., Andersson, U. B., & Eklund, O. (Eds.). (2004). *The Transscandinavian Igneous Belt (TIB) in Sweden: A review of its character and evolution*. Geological Survey of Finland.

Hrouda, F., Chlupáčová, M., & Chadima, M. (2009). *The use of magnetic susceptibility of rocks in geological exploration: Case histories study*.

Johansson, Å. (1988). The age and geotectonic setting of the Småland-Värmland granite-porphyry belt. *Geologiska Föreningen i Stockholm Förhandlingar*, *110*(2), 105–110. https://doi.org/10.1080/11035898809452648

Johansson, R., Kornfält, K.-A., Lindén, A. H., Svantesson, S.-I., Wahlgren, C.-H., Isaksson, H., & Lindroos, H. (n.d.). *Jordarter, bergarter och deformationszoner*.

Lahtinen, R., Korja, A., & Nironen, M. (2005). Paleoproterozoic tectonic evolution: Chapter 11. In M. Lehtinen, P. Nurmi, & O. T. Rämö (Eds.), *Precambrian Geology of Finland* (pp. 481–532). Elsevier Scientific Publ. Co.

Mansfeld, J. (2024). *Geology of Sweden – Bedrock Tour 24: Excursionsguide, Sveriges geologi*. Institutionen för geologiska vetenskaper, Stockholms universitet.

Mansfeld, J., Beunk ,Frank F., & and Barling, J. (2005). 1.83—1.82 Ga formation of a juvenile volcanic arc—Implications from U—Pb and Sm—Nd analyses of the Oskarshamn-Jönköping Belt, southeastern Sweden. *GFF*, *127*(2), 149–157. https://doi.org/10.1080/11035890501272149

Mansfeld, J., & Sturkell, E. F. F. (1996). Geological and geophysical investigation of a major shear zone in southeastern Sweden. *GFF*. https://doi.org/10.1080/11035899609546282

Milord, I., & Sawyer, E. W. (2003). Schlieren formation in diatexite migmatite: Examples from the St Malo migmatite terrane, France. *Journal of Metamorphic Geology*, *21*(4), 347–362. https://doi.org/10.1046/j.1525-1314.2003.00447.x

Min Karta. (n.d.). Retrieved June 18, 2025, from https://minkarta.lantmateriet.se/

Rontakokko, N., & Mansfeld, J. (2000). *Berggrundskarta Virserum*. Sveriges geologiska undersökning (SGU).

Rutanen, H. (2010, March 26). *Mantle- and crust-derived magmatism in the southern Fennoscandian Shield at c. 1.8 Ga; evidence from geochemistry, isotopes and geochronology*. Åbo Akademi - Åbo Akademi University. https://www.doria.fi/handle/10024/59511

Salin, E., Woodard, J., & Sundblad, K. (2021). Tracing the SW border of the Svecofennian Domain in the Baltic Sea region: Evidence from petrology and geochronology from a granodioritic migmatite. *International Journal of Earth Sciences*, *110*(3), 1027–1047. https://doi.org/10.1007/s00531-021-02005-z

SGUs Kartvisare. (n.d.). Retrieved June 18, 2025, from https://apps.sgu.se/kartvisare/kartvisare-berg-50-250-tusen.html

Wolf, M., Romer, R. L., Franz, L., & López-Moro, F. J. (2018). Tin in granitic melts: The role of melting temperature and protolith composition. *Lithos*, *310–311*, 20–30. https://doi.org/10.1016/j.lithos.2018.04.004

8. APPENDIX A – Field and Petrographic Data

Table A.1 *lists the outcrops from the field are, including their rock type, structural measurements (strike and dip), magnetic measurements and SWEREF 99 coordinates. The table is the groundwork for the geological map (Figure 16/17).*

Outcrop label	Rock type	Strike and dip	Susceptibility	Cord SWEREF 99 TM	Extra
LV25001	Old granitoid	017/84		0532933 6342262	Xenoliths occurs
LV25002	Old granitoid	029/81		0632961 6342211	
LV25003	Old granitoid	027/85		0532969 6342176	
LV25004	Old granitoid	040/75		0532987 6342154	
LV25005	Old granitoid	061/82		0532904 6342041	
LV25006	Intermediate Växjö granite	068/80	1500-2000	0532403 6342051	
LV25007	Gabbro (composite dike)	Contact 091/53	Gabbro 20000	0532361 6342087	
LV25008	Gabbro	Dike N/S	4000	0532313 6342086	
LV25009	Gabbro	Dike 026		0532311 6342095	
LV25010	Gabbro	Dike 019	1500-4000	0532313 6342151	
LV25011	Intermediate Växjö granite			0532310 6342182	Several outcrops of same geology.
LV25012	Gabbro	Dike N/S	15000	0532327 6341956	
LV25013	Gabbro	Dike 004	15000	0532373 6341952	
LV25014	Gabbro	Dike 017	4000-5000	0532185 6341891	
LV25015	Gabbro	Dike 010		0532187 6341811	
LV25016	Fine crystalline intermediate anatectic melt		2000-5000	0533271 6342371	

LV25017	Fine crystalline intermediate anatectic melt and Växjö granite	Oldest 154/255 Younger 109/84 Yung 120/262	Younger 2500-3500 Yung 3000	0533214 6342601	
LV25018	Växjö granite	149/260	2000-3000	0533243 6342604	
LV25019	Växjö granite	178/260		0533311 6342700	
LV25020	Växjö granite	149/267		0533313 6342776	
LV25021	Växjö granite	148/264		0533234 6342799	
LV25022	Växjö granite	146/259		0533179 6342777	
LV25023	Växjö granite	140/260	4000-5000	0533069 6342837	
LV25024	Växjö granite	148/263	3000-4000	0533127 6343003	
LV25025	Växjö granite		3000	0532993 6343210	
LV25026	Växjö granite	139/266	4000	0532863 6343205	
LV25027	Växjö granite	147/262	3000-4000	0532920 6343085	
LV25028	Växjö granite	150	3500-4500	0532862 6342986	
LV25029	Gabbro and Fine crystalline granitic anatectic melt	Parallel bedding 052/86	1000-8000	0532714 6342867	
LV25030	Fine crystalline granitic anatectic melt	174/262	1500-3000	0532764 6342844	
LV25031	Intermediate Växjö granite		1500-2000	0532181 6341871	
LV25032	Intermediate Växjö granite	021/77	1000-1500	0532443 6342003	
LV25033	Fine crystalline pink dike	Dike 161	1500	0532466 6341969	

LV25034	Gabbro	Dike 161	3000-4500	0532481 6341972	
LV25035	Intermediate Växjö granite	020/75	500-1500	0532559 6342046	
LV25036	Intermediate Växjö granite	013/78	1500	0532610 6341972	
LV25037	Gabbro	Dike 107	500-6000	0532689 6341832	
LV25038	Intermediate Växjö granite		1000-1500	0532847 6341965	
LV25039	Old granitoid	018	1500	0532819 6342088	
LV25040	Old granitoid	040/52	2500-3000	0532773 6342209	
LV25041	Old granitoid	Shear 018/264	2000-2500	0532682 6342186	
LV25042	Fine crystalline granitic anatectic melt			0533158 6342322	
LV25043	Växjö granite		4000-4500	0532969 6342870	
LV25044	Fine crystalline granitic anatectic melt		2000	0532841 6342740	
LV25045	Fine crystalline granitic anatectic melt	Layering 018	2000-3000	0532778 6342821	
LV25046	Fine crystalline granitic anatectic melt		2000-3000	0532782 6342682	
LV25047	Fine crystalline granitic anatectic melt and gabbro	Contact 129		0532708 6342649	
LV25048	Fine crystalline		1000-2000	0532640 6342650	

	pink Växjö granite				
LV25049	Fine crystalline granitic anatectic melt		1000-2000	0532532 6342735	
LV25050	Fine crystalline granitic anatectic melt		2000-3000	0532555 6342802	
LV25051	Fine crystalline pink Växjö granite		2000	0532375 6342963	
LV25052	Fine crystalline granitic anatectic melt and gabbro	Contact	Gabbro 100 Felsic 400	0532332 6342836	
LV25053	Fine crystalline granitic anatectic melt			0532344 6342619	
LV25054	Småland dike porphyry contact to gabbro	Porphyry deformation 137 Dike 155		0532377 6342603	
LV25055	Gabbro			0532493 6342573	
LV25056	Gabbro			0532435 6342680	
LV25057	Old granitoid	070	1000-4000	0532315 6342550	
LV25058	Gabbro			0532288 6342516	
LV25059	Småland dike porphyry	147		0532408 6342469	
LV25060	Gabbro, old granitoid and Fine crystalline granitic			0532466 6342473	

	anatectic melt				

Table A.2 *shows magnetic susceptibility and density measurements for selected samples.*

Sample	Susceptibility	Weight in air (grams)	Weight in water (grams)	Weight in air 2 (grams)	Density (g/cm^3)
LV25040	3000-3500	5416,9	3439,4	5421,5	2,739
LV25042	1500	4386,8	2728,6	4388,3	2,646
LV25015B	2000-3000	2840,6	1887,5	2841,0	2,980
LV25015A	30000-40000	3191,4	2106,5	3200,2	2,942
LV25016	2000-8000	5188,5	3249,3	5192,1	2,676
LV25041	1500-2500	4117,6	2617,5	4120,5	2,745
LV25007A	1000-2000	3543,4	2188,4	3545,5	2,615
LV25007B	15000-20000	4191,2	2780,4	4191,5	2,971